Finite-width effects on threshold corrections to squark and gluino production

P. Falgari,[a] **C. Schwinn**[b] **and C. Wever**[a]

[a] *Institute for Theoretical Physics and Spinoza Institute, Utrecht University,*
3508 TD Utrecht, The Netherlands

[b] *Albert-Ludwigs Universität Freiburg, Physikalisches Institut,*
D-79104 Freiburg, Germany

E-mail: P.Falgari@uu.nl, christian.schwinn@physik.uni-freiburg.de, C.S.P.Wever@uu.nl

ABSTRACT: We study the implication of finite squark and gluino decay widths for threshold resummation of squark and gluino production cross sections at the LHC. We find that for a moderate decay width ($\Gamma/\bar{m} \lesssim 5\%$) higher-order soft and Coulomb corrections are appropriately described by NLL calculations in the zero-width limit including the contribution from bound-state resonances below threshold, with the remaining uncertainties due to finite-width effects of a similar order as the ambiguities of threshold-resummed higher-order calculations.

Contents

1 Introduction

A recent development in the effort to improve theoretical predictions for the pair production of squarks and gluinos at hadron colliders has been the calculation of higher-order threshold corrections in QCD [1–12], i.e. corrections that are enhanced in the limit of a small relative velocity β of the produced squark/gluino pair

$$\beta \equiv \sqrt{1 - \frac{4\bar{m}^2}{\hat{s}}} \to 0, \tag{1.1}$$

with the partonic centre-of-mass energy $\hat{s}$ and the average mass $\bar{m}$ of the sparticle pair. These threshold corrections are given by two contributions, Coulomb corrections, that occur in powers of α_s/β, and threshold logarithms of the form $\alpha_s^n \ln^m \beta$. In the limit (1.1), the expansion in the strong coupling constant must be reorganized, since both types of corrections can become of order one,

$$\alpha_s \ln \beta \sim 1 , \quad \frac{\alpha_s}{\beta} \sim 1. \tag{1.2}$$

Resumming all enhanced contributions to all orders using eikonal methods [13–16] and non-relativistic field theory [17], the cross section assumes the form

$$\hat{\sigma}_{pp'} \propto \hat{\sigma}^{(0)} \sum_{k=0}^{\infty} \left(\frac{\alpha_s}{\beta} \right)^k \exp \Big[\underbrace{\ln \beta \, g_0(\alpha_s \ln \beta)}_{(\text{LL})} + \underbrace{g_1(\alpha_s \ln \beta)}_{(\text{NLL})} + \underbrace{\alpha_s g_2(\alpha_s \ln \beta)}_{(\text{NNLL})} + \dots \Big]$$

$$\times \left\{ 1 \, (\text{LL,NLL}); \alpha_s, \beta \, (\text{NNLL}); \alpha_s^2, \alpha_s \beta, \beta^2 \, (\text{NNNLL}); \dots \right\}. \qquad (1.3)$$

For squark and gluino production, the corrections beyond next-to-leading order (NLO) can be large, becoming as large as the NLO cross sections for the case of heavy gluinos.

In the calculations of threshold corrections the produced squarks and gluinos are usually treated as stable, while in most realistic SUSY models they are highly unstable and decay promptly.[1] In a more realistic treatment including finite decay widths Γ, the threshold singularities are smoothed [17] since the decay width sets the smallest perturbative scale in the process. This raises the question of whether the resummation based on the counting (1.2) is appropriate in the presence of the new scale Γ and to which extent the large higher-order threshold corrections found for stable squarks and gluinos provide a reasonable approximation to the more realistic unstable case. One effect of the finite decay width is the emergence of a non-vanishing partonic cross section below the nominal production threshold $\hat{s} = 4\bar{m}^2$, as discussed for stop-pair production in [20], and more recently for gluino pair [21, 22] and squark-gluino production [23]. In our previous combined resummation of threshold logarithms and Coulomb corrections for squark and gluino pair-production [11, 12] the contribution from the region below the nominal threshold to the total production cross section has been taken into account in the zero-width limit, where the smooth invariant-mass distribution turns into a series of would-be bound-state poles.

As we will show in this note, for moderate decay widths $\Gamma/\bar{m} \lesssim 5\%$, the finite-width effects on higher-order QCD corrections are small and within the error estimate of the NLL cross sections with soft and Coulomb resummation and bound-state corrections. This covers the relevant production channels in the MSSM, since larger decay widths only arise for heavier gluinos with a large gluino-squark mass splitting, in which case gluino production is suppressed compared to squark production. Therefore the treatment of NLL soft and Coulomb corrections in [12] captures the dominant higher-order QCD effects also when the instability of squarks and gluinos is taken into account. Furthermore, the dominant effect of the finite decay widths arises at NLO, so the impact on higher-order corrections is small.

It should be emphasized that the aim of our study is the assessment of finite-width effects on QCD corrections beyond LO rather than a complete treatment at leading and next-to-leading order. Studies of other aspects of finite squark and gluino decay widths include that of non-resonant tree diagrams [24]; the accuracy of the narrow-width approximation for small mass-splittings of the decaying particle and its decay products [25, 26], the consistent treatment of off-shell effects in Monte-Carlo programs [27] and NLO corrections to production and decay for the squark-squark production process [28].

---

[1] We do not consider the case of stops and gluinos that are stable on collider timescales. For recent work on higher-order corrections in this case see [18, 19].

This article is organized as follows. In section 2 we specify the considered production and decay processes and review the effective-theory treatment of unstable particles [29–32] and soft and Coulomb resummation near threshold [11]. In section 3 we estimate the impact of the screening of threshold corrections by the finite decay width as well as the magnitude of non-resonant corrections. In section 4 we study the invariant-mass spectrum for squark and gluino production processes at the LHC and the total production cross sections. We find that for moderate decay widths the finite-width corrections to the total cross section are within the residual uncertainty of the NLL calculation of [12].

2 Theoretical framework

2.1 Production and decay of squarks and gluinos in SQCD

In this note we consider the pair-production processes of squarks $\tilde{q}$ and gluinos $\tilde{g}$ at hadron colliders in supersymmetric QCD (SQCD) that proceed through the partonic production channels

$$pp' \to \tilde{s}_1\tilde{s}_2X \ , \tag{2.1}$$

where $\tilde{s}_i \in \{\tilde{q}, \bar{\tilde{q}}, \tilde{g}\}$ denote the two produced sparticles and $p, p' \in \{q, \bar{q}, g\}$ the initial-state partons. The average mass of the sparticle pair is given by

$$\bar{m} = \frac{m_{\tilde{s}_1} + m_{\tilde{s}_2}}{2}. \tag{2.2}$$

In general, the produced squarks and gluinos can decay via long cascade decay chains to a final state of standard model particles and the lightest supersymmetric particle (assuming the latter is stable on detector time scales). For this initial study of finite-width effects we limit ourselves to squark and gluino decay in pure SQCD, i.e. we neglect the decay width of the lightest coloured sparticle and consider the decay modes

$$\begin{aligned} \tilde{q} \to q\tilde{g}, \quad \bar{\tilde{q}} \to \bar{q}\tilde{g}, \quad m_{\tilde{q}} > m_{\tilde{g}}, \\ \tilde{g} \to q\bar{\tilde{q}}, \quad \tilde{g} \to \bar{q}\tilde{q}, \quad m_{\tilde{q}} < m_{\tilde{g}}. \end{aligned} \tag{2.3}$$

We treat the masses of the different squark flavours as degenerate and equal to $m_{\tilde{q}}$, while the gluino mass equals $m_{\tilde{g}} \neq m_{\tilde{q}}$. The full one-loop SUSY-QCD partial widths of the above decay processes have been calculated in [33]. The NLO corrections to the LO partial widths were found to be of the order of $30 - 50\%$ and will not be given here. In order to estimate the finite-width effects we will employ the LO tree level SUSY-QCD widths,

$$\Gamma(\tilde{q} \to q\tilde{g}) = \frac{\alpha_s C_F m_{\tilde{q}}}{2}\Big(1 - \Big(\frac{m_{\tilde{g}}}{m_{\tilde{q}}}\Big)^2\Big)^2, \ m_{\tilde{q}} > m_{\tilde{g}},$$

$$\Gamma(\tilde{g} \to q\bar{\tilde{q}}, \bar{q}\tilde{q}) = \frac{\alpha_s n_f m_{\tilde{g}}}{2}\Big(1 - \Big(\frac{m_{\tilde{g}}}{m_{\tilde{q}}}\Big)^{-2}\Big)^2, m_{\tilde{q}} < m_{\tilde{g}}. \tag{2.4}$$

Since the numerical values are only used for illustration of the finite-width effects, we only consider gluino decay into light-flavour and bottom squarks that are treated as mass-degenerate, i.e. we set $n_f = 5$. Therefore we neglect the decay into stops and the related

additional dependence on the parameters of the stop sector unless stated otherwise. The effect of gluino decay to stops on our results is discussed briefly in section 4.2. In the full MSSM, the lighter coloured sparticles are, of course, unstable with respect to electroweak two- or three-body decays $\tilde{q} \to \chi q$ and $\tilde{g} \to q\bar{q}\chi$ for charginos or neutralinos χ, which have been calculated in leading order in [34, 35] and for which state-of-the-art predictions are implemented in [36–39]. These effects would be straightforward to include in our framework but would introduce a dependence on the electroweak parameters of the MSSM. Therefore we will use the tree-level SQCD decay widths (2.4) for the purpose of estimating the size of finite-width effects in higher-order QCD corrections. Since the electroweak decay widths are typically of the order $\Gamma/\bar{m} < 1\%$, this should not affect our qualitative conclusions. We therefore consider production and decay processes of squarks and gluinos at hadron colliders of the type

$$pp' \to \tilde{s}_1\tilde{s}_2 \to (\tilde{s}'_1 p_1)\,(\tilde{s}'_2 p_2), \tag{2.5}$$

with massless partons $p_{1/2}$. Such four-body final states arise in SQCD for gluino pair production for the case $m_{\tilde{g}} > m_{\tilde{q}}$ or squark-(anti-)squark production for $m_{\tilde{q}} > m_{\tilde{g}}$. The treatment of a three-body final state that arises for squark-gluino production in our approximation should be obvious. In detail, the partonic production and decay processes of squarks and gluinos for the two mass hierarchies are as follows:

$$
\begin{aligned}
m_{\tilde{g}} < m_{\tilde{q}} : \qquad\qquad & gg, q_i\bar{q}_i \to \tilde{g}\tilde{g}, \\
& q_i g \to \tilde{q}\tilde{g} \to q\tilde{g}\tilde{g}, \\
& gg, q_i\bar{q}_j \to \tilde{q}\bar{\tilde{q}} \to q\bar{q}\tilde{g}\tilde{g}, \\
& q_i q_j \to \tilde{q}\tilde{q} \to qq\tilde{g}\tilde{g}, \\
m_{\tilde{g}} > m_{\tilde{q}} : \qquad\qquad & gg, q_i\bar{q}_j \to \tilde{q}\bar{\tilde{q}}, \\
& q_i q_j \to \tilde{q}\tilde{q}, \\
& q_i g \to \tilde{q}\tilde{g} \to \bar{q}\tilde{q}\tilde{q}, \\
& gg, q_i\bar{q}_i \to \tilde{g}\tilde{g} \to \bar{q}\bar{q}\tilde{q}\tilde{q}
\end{aligned}
\tag{2.6}
$$

where $i, j = u, d, s, c, b$ and all charge conjugated processes are understood.

The complete gauge-invariant set of Feynman diagrams for the production of the three- or four-body final states of "stable" particles (2.6) contain doubly-resonant diagrams, i.e. diagrams where the particles indicated in the first step of (2.6) appear as internal lines, and singly- or non-resonant diagrams, where only one or none of the unstable squarks or gluinos is present. Examples of these topologies are given in figure 1. Beyond leading order, the production processes cannot be strictly separated since, e.g. the process $q_i g \to \bar{q}\tilde{q}\tilde{q}$ enters the real NLO corrections to $\tilde{q}\tilde{q}$-production. Furthermore, the non-resonant diagrams can contain collinear singularities (e.g. the last topology given in figure 1) that would cancel against higher-order virtual corrections and require taking kinematic cuts on the final state particles into account.

A full NLO QCD calculation of a process comparable to (2.5) including finite-width effects has been performed in the standard model for the case of $b\bar{b}W^+W^-$ production [40, 41], but not yet for an MSSM process. Very recently, a tool for automatic calculation of
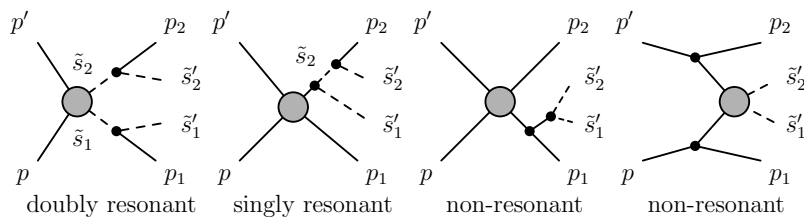
Figure 1. Examples of Feynman-diagram topologies contributing to the generic production and decay process (2.5). The second non-resonant diagram contains collinear singularities.

MSSM processes at NLO has been presented in [42], but so far applied to the on-shell processes (2.1). Short of a full NLO calculation, a well-defined approximation method for calculating radiative corrections to production and decay processes is based on the pole expansion [43, 44]. In this framework the total partonic production cross sections for the processes (2.6) is written in the form

$$\hat{\sigma}_{pp'}(\hat{s}) = \hat{\sigma}_{pp'}^{\mathrm{res}}(\hat{s}) + \hat{\sigma}_{pp'}^{\mathrm{non\text{-}res}}(\hat{s}). \tag{2.7}$$

The doubly-resonant cross-section $\hat{\sigma}^{\mathrm{res}}$ is defined in a consistent way by an expansion of the S-matrix around the complex poles of the Dyson-resummed propagators of the unstable particles [43, 44]. At NLO it contains both factorizable corrections to production and decay, as well as non-factorizable corrections connecting production, propagation and decay stages. Non-factorizable corrections related to the final state cancel for the total cross section [45, 46], but not for differential distributions. The fully differential factorizable corrections to production and decay have recently been computed for squark-squark production [28]. For the remaining processes, at present only the corrections to the total production cross sections [47] and decay rates [33] are available. The "non-resonant" cross-section $\hat{\sigma}^{\mathrm{non\text{-}res}}$ includes singly- and non-resonant Feynman-diagrams as well as contributions from doubly-resonant diagrams where one or both of the $\tilde{s}_1$ or $\tilde{s}_2$ lines are far off-shell.

2.2 Effective theory framework for unstable particles

For the investigation of the interplay of higher-order threshold corrections in QCD and finite squark and gluino lifetimes, we are interested in the partonic cross sections for the processes (2.6) near the partonic production threshold (1.1). For the precise definition of the resonant and non-resonant contributions to the cross section we adopt the effective-theory approach to unstable particles [29, 30], generalizing the treatment of W-boson pair production at an electron positron collider [31, 32]. The aim of the effective-theory approach is to provide a precise prediction of the partonic cross section for partonic centre-of-mass energies in the vicinity of the threshold, $\hat{s} - 4\bar{m}^2 \sim \bar{m}\Gamma$. This is achieved by a simultaneous expansion in the quantity

$$\delta = \frac{\hat{s} - 4\bar{m}^2}{\bar{m}^2} \approx \beta^2 \tag{2.8}$$

and the coupling constants. For power-counting purposes, we therefore set

$$\beta \sim (\Gamma/\bar{m})^{1/2} \sim \delta^{1/2}. \tag{2.9}$$

Figure 2. Diagrammatic representation of the leading resonant and non-resonant contribution to the forward-scattering amplitude in unstable-particle effective theory.
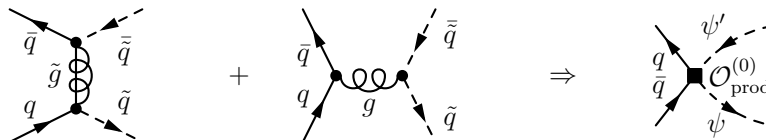

Figure 3. Computation of the matching coefficient of the production operator for squark-antisquark production from the quark-antiquark initial state.
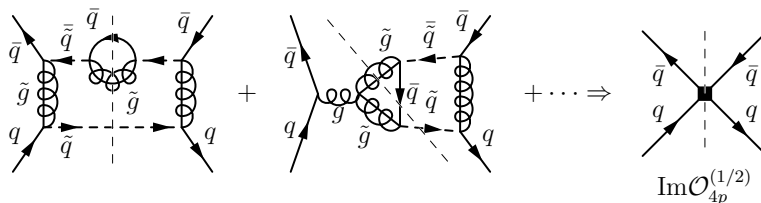

Figure 4. Computation of the matching coefficient of the four-parton operator for squark-antisquark production and decay. The first diagram is an example of a double-resonant diagram, the second of the interference of a double-resonant and a single-resonant diagram.

The leading-order resonant production cross-section for S-wave production processes is of the form

$$\hat{\sigma}_{pp'}^{\text{res}}(\hat{s}, \mu) \sim \alpha_s^2 \beta. \tag{2.10}$$

Near the production threshold, the processes (2.5) can be treated in an effective theory where the light-partons are described by collinear fields ϕ, ϕ' in soft-collinear effective theory (SCET) [48–50] and the pair-produced squarks and gluinos are described by non-relativistic fields ψ, ψ' in potential non-relativistic QCD (pNRQCD) [51]. In the leading effective Lagrangian, the collinear and non-relativistic fields interact only through the exchange of soft gluons, which give rise to the non-factorizable corrections mentioned above. This effective theory has also been used for soft-gluon and Coulomb resummation in [11], where more details can be found.

In the EFT framework, the total partonic cross section for the process (2.5) is computed from the imaginary part of the partonic forward-scattering amplitudes $\mathcal{A}_{pp'}$ of the processes $pp' \to pp'$ which reads[2]

$$i\mathcal{A}_{pp'}(\hat{s})|_{\hat{s}\sim 4\bar{m}^2} = \int d^4x \, \langle pp'|T\left[i\mathcal{O}_{\text{prod}}^{\dagger}(0)i\mathcal{O}_{\text{prod}}(x)\right]|pp'\rangle + \langle pp'|i\mathcal{O}_{4p}(0)|pp'\rangle . \tag{2.11}$$

---

[2]As written, the forward-scattering amplitude is not infrared safe but requires mass factorization where matrix elements of the collinear fields are identified with parton distribution functions (PDFs).

The "production operator" $\mathcal{O}_{\mathrm{prod}} = C_{\mathrm{prod}}\, \phi\phi'\, \psi^\dagger \psi'^\dagger$ describes the resonant production of the $\tilde{s}_1 \tilde{s}_2$-pair from pp' collisions while the expectation value of the four-parton operators $\mathcal{O}_{4p} = C_{4p}\, \phi^\dagger \phi'^\dagger \phi \phi'$ describes the non-resonant contributions. The two terms in (2.11) therefore correspond to the resonant and non-resonant cross sections defined earlier in (2.7), see figure 2. The cross section for a specific final state $\tilde{s}_1' \tilde{s}_2' p_1 p_2$ can be obtained by computing the imaginary part of the forward-scattering amplitude using unitarity cuts and selecting only cuts corresponding to the desired final state [31]. At leading order, this simply amounts to multiplying by the branching ratios $\mathrm{BR}(\tilde{q}_1 \to \tilde{q}_1' p_1)$ and $\mathrm{BR}(\tilde{q}_2 \to \tilde{q}_2' p_2)$. The matching coefficients C_{prod} of the production operators are computed from the on-shell amplitude for the processes $pp' \to \tilde{s}_1 \tilde{s}_2$ at the desired accuracy, as sketched for LO in figure 3. The coefficients C_{4p} are calculated by expanding the forward-scattering amplitude in the hard momentum region, where all loop momenta are far off-shell.[3] The leading non-resonant contribution to the processes (2.5) arises from the squared tree amplitudes of the processes $pp' \to \tilde{s}_1 \tilde{s}_2' p_2$ and $pp' \to \tilde{s}_1' p_1 \tilde{s}_2$ as sketched in figure 4 for the example of squark-antisquark production and decay. The EFT calculation of the forward-scattering amplitude to order α_s and δ includes soft one-loop corrections, the one-loop corrections to C_{prod} as well as kinematic corrections due to subleading kinetic Lagrangian terms.

2.3 Soft and Coulomb resummation for the resonant contributions

The resummation of soft logarithms and Coulomb corrections has been derived in [11] by establishing a factorization of the doubly resonant contribution to the partonic cross section into hard, soft and non-relativistic (potential) matrix elements,

$$\hat{\sigma}_{pp'}^{\mathrm{res}}(\hat{s}, \mu) = \sum_{R_\alpha} H_{pp'}^{R_\alpha}(m_{\tilde{q}}, m_{\tilde{g}}, \mu) \int d\omega\, J_{R_\alpha}\!\left(E + i\,\bar{\Gamma} - \frac{\omega}{2}\right) W^{R_\alpha}(\omega, \mu). \tag{2.12}$$

Here we have defined the average width

$$\bar{\Gamma} = \frac{1}{2}(\Gamma_{\tilde{s}_1} + \Gamma_{\tilde{s}_2}) \tag{2.13}$$

and R_α are the irreducible colour representations in the decomposition of the product of the colour representations of the sparticles $\tilde{s}_1$ and $\tilde{s}_2$. In analogy to the zero-width treatment in [12], as a default we use the expression

$$E = \bar{m}\left(1 - \frac{4\bar{m}^2}{\hat{s}}\right) \tag{2.14}$$

for the energy of the squark or gluino pair which coincides with the non-relativistic expression $E = \bar{m}\beta^2$ for $\hat{s} > 4\bar{m}^2$. Therefore we refer to this treatment as the 'β-implementation'. In order to estimate ambiguities of the threshold approximation we will also use an 'E-implementation' defined by $E = \sqrt{\hat{s}} - 2\bar{m}$ that agrees with (2.14) near threshold.

The hard functions $H_{pp'}^{R_\alpha}$ are related to the square of the matching coefficients C_{prod}. At LO they are proportional to the Born cross section at threshold.[4] The soft functions W^{R_α}

---

[3]Explicit calculations have been performed for W-pair production [31] and top-pair production [52, 53] at electron-positron colliders.

[4]As in [12], in our numerical results we compute the hard function from the full Born cross section instead of its threshold limit.

are matrix elements of soft-gluon Wilson lines and implement the eikonal approximation. Precise definitions can be found in [11]. Threshold resummation of soft logarithms can be performed using renormalization group equations for the hard and soft function [9, 54, 55] that can be solved in Mellin-moment or momentum space [56]. The relevant anomalous dimensions for all squark and gluino production processes up to NNLL accuracy have been collected in [9, 11].

The potential function J_{R_α} is an expectation value of the non-relativistic fields $\psi^{(0)}$, that have been decoupled from the soft gluons by a field redefinition and interact only through the exchange of Coulomb gluons. It is related to the zero-distance Green function of the non-relativistic Schrödinger equation with a Coulomb potential, $G_{\mathrm{C}}^{R_\alpha(0)}(0,0;\mathcal{E})$:

$$J^{R_\alpha}(\mathcal{E}) = 2\,\mathrm{Im}\,G_{\mathrm{C}}^{R_\alpha(0)}(0,0;\mathcal{E})\,, \tag{2.15}$$

with the Coulomb Green function including all-order gluon exchange in the $\overline{\mathrm{MS}}$-scheme [57, 58]:

$$G_{\mathrm{C}}^{R_\alpha(0)}(0,0;\mathcal{E}) = -\frac{(2m_{\mathrm{red}})^2}{4\pi}\left\{\sqrt{-\frac{\mathcal{E}}{2m_{\mathrm{red}}}} + (-D_{R_\alpha})\alpha_s\left[\frac{1}{2}\ln\left(-\frac{8\,m_{\mathrm{red}}\mathcal{E}}{\mu^2}\right)\right.\right.$$
$$\left.\left. -\frac{1}{2} + \gamma_E + \psi\left(1 - \frac{(-D_{R_\alpha})\alpha_s}{2\sqrt{-\mathcal{E}/(2m_{\mathrm{red}})}}\right)\right]\right\}. \tag{2.16}$$

Here γ_E is the Euler-Mascheroni constant and $m_{\mathrm{red}} = m_{\tilde{s}_1}m_{\tilde{s}_2}/(m_{\tilde{s}_1} + m_{\tilde{s}_2})$. The coefficients $D_{R_\alpha} = \frac{1}{2}(C_{R_\alpha} - C_{R_1} - C_{R_2})$ of the Coulomb potential depend on the quadratic Casimir operators of the colour representations R_i of the sparticles $\tilde{s}_i$ and of the irreducible representation R_α in the decomposition of $R_1 \otimes R_2$. The trivial ($\alpha_s \to 0$) potential function for finite width obtained by neglecting the Coulomb corrections is given by

$$J^{R_\alpha(0)}(E + i\bar{\Gamma}) = \frac{\sqrt{2}m_{\mathrm{red}}^{3/2}(E^2 + \bar{\Gamma}^2)^{1/4}}{\pi}\frac{E + (E^2 + \bar{\Gamma}^2)^{1/2}}{\sqrt{\left(E + (E^2 + \bar{\Gamma}^2)^{1/2}\right)^2 + \bar{\Gamma}^2}}. \tag{2.17}$$

The use of a complex energy $E + i\bar{\Gamma}$ takes the finite-width effects in the doubly-resonant cross section into account in leading order in the non-relativistic expansion [17].

For energies below the production threshold $E < 0$ and for $\bar{\Gamma} = 0$, the Coulomb Green function develops a series of bound-state poles at energies

$$E_n = -\frac{2m_{\mathrm{red}}\alpha_s^2 D_{R_\alpha}^2}{4n^2}\,. \tag{2.18}$$

These contributions have been taken into account in the NLL predictions of [12]. For unstable particles, the complex energy shift in the potential function in (2.12) leads to a smoothing of the discrete set of bound-state poles (2.18) into a continuous non-vanishing contribution below the nominal production threshold.

3 Estimate of contributions to the cross section

In section 2 we have discussed the treatment of finite-width effects (section 2.2) and higher-order soft and Coulomb corrections for the case of stable particles (section 2.3). The resummation of threshold logarithms and Coulomb corrections was performed under the assumption (1.2) that a sizable contribution to the total hadronic cross section arises from the region where $\alpha_s \ln \beta \sim \frac{\alpha_s}{\beta} \sim 1$, leading to a reorganization of the perturbative expansion according to (1.3). For finite decay widths, the replacement $E \to E + i\bar{\Gamma}$ in the potential function leads to the screening of the threshold singularities, raising the question if the resummation based on the counting (1.2) is still justified. Furthermore, for an unstable particle the size of the non-resonant contribution to the cross section (2.7) compared to the higher-order corrections to the resonant contributions has to be addressed. In this section we use power-counting arguments to estimate these effects and compare these expectations to explicit results for squark and gluino production.

3.1 Size of the decay width

To discuss the size of the screening effect and the non-resonant contributions, we consider the decay of the sparticle $\tilde{s}$ of mass M into a sparticle $\tilde{s}'$ of mass m and a massless parton p, mediated by the strong interaction. On kinematic grounds, the decay width is of the form

$$\Gamma(\tilde{s} \to \tilde{s}'p) = \alpha_s M \left(1 - x^2\right) f(x) \tag{3.1}$$

for some function f of the mass ratio

$$x \equiv \frac{m}{M}. \tag{3.2}$$

In the following, we consider the decay width (3.1) for two limiting cases:

a) Light decay product, $x \to 0$:

$$\Gamma/M \sim \alpha_s. \tag{3.3}$$

In this case, the expansion parameter δ of the effective theory (2.9) is estimated as

$$\delta \sim \beta^2 \sim \alpha_s. \tag{3.4}$$

b) Heavy decay product, $x \to 1$:

$$\Gamma/M \sim \alpha_s \times (1 - x^2)^\gamma, \tag{3.5}$$

where $\gamma = 1$ if the function $f(x)$ in (3.1) is of the order one, but $\gamma = 2$ for the case of squark and gluino decay (2.4). In this case, another small scale $\kappa \equiv (1-x^2)^\gamma$ is present, and the hierarchy of scales is given by

$$\delta \sim \beta^2 \sim \alpha_s \kappa. \tag{3.6}$$

In particular, if for squarks and gluinos the numerical size of the mass ratio is such that $\kappa = (1 - (m/M)^2)^2 \sim 0.1$, i.e. $m/M \gtrsim 0.8$, we count $\delta \sim \alpha_s^2$.
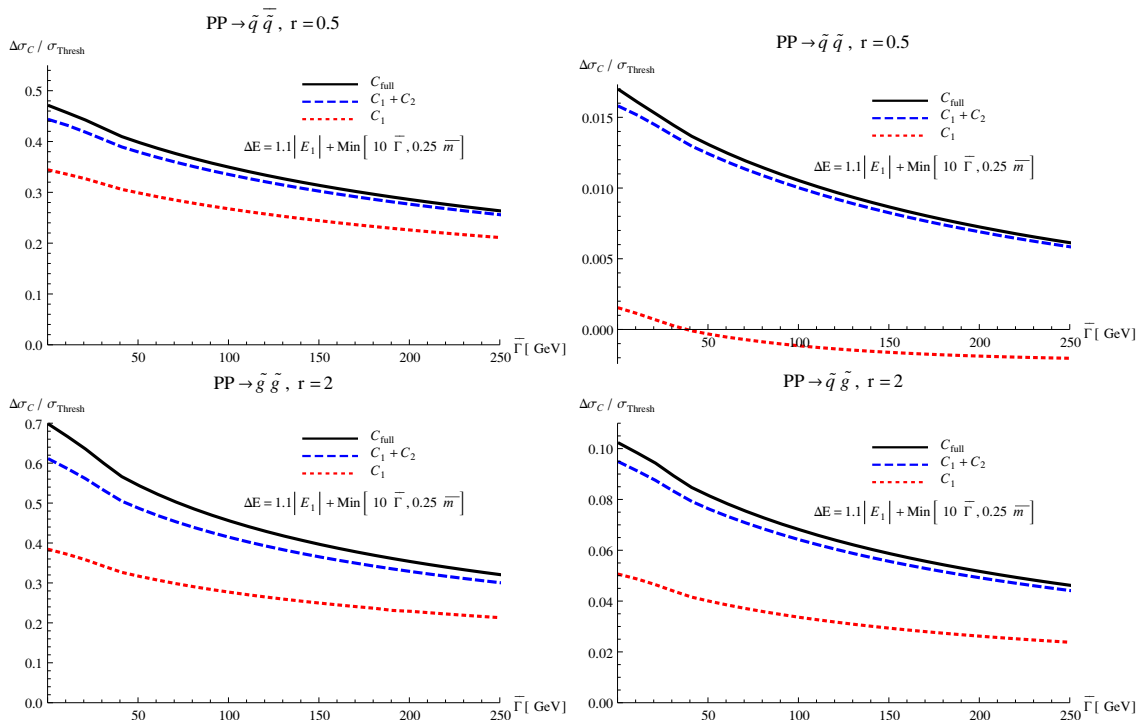
Figure 5. Size of the first Coulomb correction (red, dotted), first and second Coulomb corrections (blue, dashed) and resummed Coulomb corrections (black, solid) relative to the leading cross section in the effective theory as a function of $\bar{\Gamma}$ and for $\bar{m} = 1500\,\text{GeV}$ at the LHC with $\sqrt{s} = 8\,\text{TeV}$. r is defined as $r = m_{\tilde{g}}/m_{\tilde{q}}$. For technical reasons the potential function is set to zero for $E < \Delta E$ as defined in (4.6).

For the phenomenology of unstable strongly-interacting particles, different scenarios have been identified (e.g. [21, 59]). For very narrow particles, bound states can form that subsequently decay into di-photon or di-jet final states and therefore lead to a very different phenomenology than the missing energy signatures usually employed in squark and gluino searches. In the MSSM this case is only relevant for gluinonium and stoponium production and will not be considered further here. For a sparticle decay width that is larger than the bound-state decay widths into di-photons or di-jets, but much smaller than the energy E_1 of the first bound-state (2.18), a few bound state-peaks can form, but the decay is dominated by the underlying sparticle decay, while for $\bar{\Gamma} \lesssim E_1$, bound-state effects enhance the cross section near threshold, but the different peaks might not be separated. Since $E_1 \sim \alpha_s^2$, bound-state peaks might be visible in the invariant-mass distribution below threshold for narrow sparticles in the category b), as we will study in section 4.1. For $\bar{\Gamma} > E_1$ the bound-state effects are washed out, which we expect to be the case for broader sparticles in category a).

We will now estimate the size of the Coulomb and soft corrections as well as the non-resonant contributions for these two limiting cases.

3.2 Coulomb corrections

In the two scenarios for the decay width, the n-th Coulomb correction is of the order

$$\left(\frac{\alpha_s}{\beta}\right)^n \sim \left(\frac{\alpha_s^2}{\delta}\right)^{n/2} \sim \begin{cases} \delta^{n/2} \sim \alpha_s^{n/2}, & \text{case a)} \\ \left(\frac{\alpha_s}{\kappa}\right)^{n/2}, & \text{case b)} \end{cases} \tag{3.7}$$

Therefore by power counting, Coulomb resummation is not necessary for case a), i.e. for particles with decay widths of the order of $\Gamma/M \sim \alpha_s \sim 10\%$. This exemplifies the screening of the threshold corrections by the finite lifetime. However, to reach NLO accuracy in $\delta \sim \alpha_s$ the second Coulomb correction has to be included. This is analogous to the case of W-pair production considered in [31] (up to the replacement of α by α_s). In the opposite limit of narrow particles where numerically $\frac{\Gamma}{M} \sim \alpha_s^2 \sim 1\%$ (case b), $\kappa \sim \alpha_s$ so the screening of the Coulomb corrections is not effective and Coulomb resummation should be performed as in the stable case.[5] Since in these formal counting arguments the numerical prefactors such as the strength of the Coulomb potential are not taken into account, the actual relevance of the Coulomb corrections has to be studied on a process-by-process basis. In figure 5 we show the contribution of the first (C_1, red dotted line) and second (C_2, blue dashed line) Coulomb corrections, as well as the resummed Coulomb corrections (C_{full}, solid black line), to the total hadronic production cross sections as a function of the decay width for all four squark and gluino production processes. The Coulomb corrections are normalized by the approximation $\sigma_{\text{Thresh}}^{(0)}$ that is defined as the effective theory cross section (2.12) without soft-gluon resummation and using only the α_s^0 term of the potential function (2.17). One sees that for larger widths the Coulomb corrections are increasingly saturated by the first two Coulomb corrections, while the second Coulomb correction always gives a non-negligible contribution, in agreement with the general discussion above. However, the total contribution of the Coulomb corrections can be sizable, as for gluino-pair production, or numerically small, as for squark-squark production.

3.3 Soft corrections

The parametric scaling of soft corrections in the scenarios a) and b) considered in section 3.1 is given by

$$\ln \beta \sim \ln \sqrt{\delta} \sim \begin{cases} \frac{1}{2} \ln \alpha_s, & \text{case a)} \\ \frac{1}{2}(\ln \alpha_s + \ln \kappa) \sim \ln \alpha_s, & \text{case b)} \end{cases} \tag{3.8}$$

where in case b) we have again considered the case where numerically $\kappa \sim \alpha_s$. It is thus not obvious at a first glance in which scenarios resummation of soft-gluon correction is necessary, if at all, since for $\alpha_s \sim 0.1$ one has $\alpha_s |\ln \alpha_s| \sim 0.23$. Clearly one would expect resummation effects to be more important for case b), where the screening effect due to a finite width is less effective. However the parametric scaling in the two scenarios is formally the same and equal, up to constant prefactors, to $\sim \ln \alpha_s$. As already stressed for the case of Coulomb corrections, the scaling argument which leads to (3.8) does not

---

[5]This is analogous to the well-known case of top-quark production at linear colliders, where the small decay width of the top is due to the electroweak nature of the decay, $\Gamma_t/m_t \sim \alpha_{\text{EW}} \sim \alpha_s^2$.
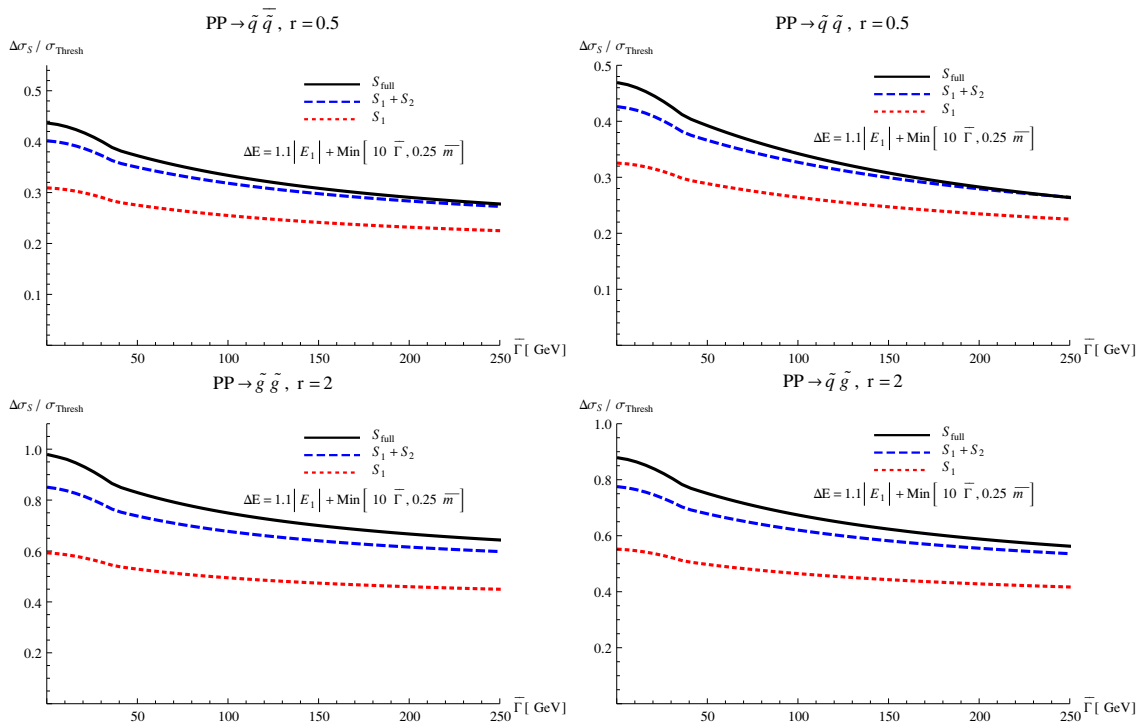
Figure 6. Size of the NLL soft corrections expanded to NLO (red, dotted), up to NNLO (blue, dashed) and the resummed NLL corrections (black, solid) relative to the leading cross section in the effective theory as a function of $\bar{\Gamma}$ and for $\bar{m} = 1500\,\text{GeV}$ at the LHC with $\sqrt{s} = 8\,\text{TeV}$. The remaining definitions are as in figure 5.

take into account the coefficients of the logs, which can be numerically large. This is particularly true for gluon-initiated squark-antisquark production and for squark-gluino and gluino-gluino production, where the Casimir invariants for the adjoint and higher colour representations appear in the prefactors. Once again, a meaningful assessment of the importance of resummation can only be done on a process-by-process basis by a numerical analysis of different fixed-order contributions.

Figure 6 shows the effect of NLL soft resummation (S_{full}, solid black line) on the cross section of the four SUSY-production processes considered in this work and the contributions of the $\mathcal{O}(\alpha_s)$ (S_1, red dotted line) and $\mathcal{O}(\alpha_s^2)$ (S_2, blue dashed line) terms obtained from the expansion of the resummed cross section, as a function of the width $\bar{\Gamma}$. As in figure 5 the cross sections are normalized to the leading threshold approximation. It can be seen that for small widths of order $\bar{\Gamma}/\bar{m} \sim \alpha_s^2$ resummation is numerically important for all processes (and more so for those where large colour charges are involved), with NNLO corrections of the order of $10-25\%$ of the LO cross section and terms beyond NNLO as large as $\sim 10\%$ for squark-gluino and gluino-gluino production. One can therefore argue that in scenario b) it makes sense to keep the zero-width scaling $\alpha_s \ln \beta \sim 1$ for soft logarithms, which leads to the representation of the cross section given in (1.3).

At larger width ($\bar{\Gamma}/\bar{m} \gtrsim \alpha_s$) the bulk of NLL corrections is accounted for by the $\mathcal{O}(\alpha_s)$ terms, which correspond to a $30-50\%$ contribution to the Born result. However NNLO

terms still represent a correction of order $5 - 15\%$ depending on the process considered. Consistent with the stronger screening effect expected for larger widths, higher-order soft corrections beyond NNLO are small, $\lesssim 5\%$ for gluino-gluino and squark-gluino production and below 1% for squark-antisquark and squark-squark production. We thus conclude that in case a) the relevance of soft resummation is not immediately clear, though the inclusion of higher-order corrections at NNLO might still be necessary to achieve an accuracy of order $\delta \sim \alpha_s$. It is interesting to note that for large widths the fixed-order one-loop soft correction is numerically about $\sqrt{\alpha_s} \sim 30\%$ of the tree-level threshold result, and the two-loop soft terms of order $(\sqrt{\alpha_s})^2 \sim 10\%$.

To summarize, in the two limiting scenarios one can give the following parametric representation of the cross section:

a) Adopting for the soft logarithms the (approximate) scaling $\alpha_s \ln^2 \beta \sim \sqrt{\delta} \sim \sqrt{\alpha_s}$, which is motivated by the numerical results in figure 6, and using (3.7), the cross section can be represented as

$$
\hat{\sigma}_{pp'} \propto \hat{\sigma}^{(0)} \times
\begin{cases}
1 & \text{LO} \\
\frac{\alpha_s}{\beta}, \alpha_s \ln^2 \beta & \text{N}^{1/2}\text{LO} \\
\alpha_s, \left(\frac{\alpha_s}{\beta}\right)^2, (\alpha_s \ln^2 \beta)^2, (\alpha_s \ln \beta)^2/\beta, \alpha_s \ln \beta, \beta^2 & \text{NLO} \\
\dots
\end{cases}
\tag{3.9}
$$

where the expansion in half-integer powers of δ is similar to the case of W-pair production at a linear collider [31]. There are no terms linear in β because they are known to average out to zero for the total cross section.

b) For the case $\kappa \sim \alpha_s$, the counting is identical to the stable case.

While according to (3.9) resummation is parametrically not necessary for $\bar{\Gamma}/\bar{m} \gtrsim \alpha_s$, in practice it is not always clear for which numerical value of $\bar{\Gamma}$ one can switch from the prescription (1.3) to (3.9). This is particularly true for the transition region where $\alpha_s^2 \lesssim \bar{\Gamma}/\bar{m} \lesssim \alpha_s$. For this reason in section 4 we will use the NLL implementation of (1.3) for arbitrary values of the width. This choice has the advantage of including, in both limits of a small and large width, all the terms relevant to achieving an accuracy of $\sim \delta$, with the exception of the β^2 contribution appearing at NLO in the counting (3.9). These are however correctly taken into account by matching the effective-theory result to the exact Born result including the leading finite-width and power suppressed effects, as explained in section 3.4.

3.4 Non-resonant corrections

We now turn to an estimate of the size of non-resonant corrections neglected in present higher-order calculations that treat squarks and gluinos as stable. The leading non-resonant contributions as well as subleading kinetic corrections to the double-resonant cross section are both included in a calculation of the full Born cross section of a process of the form (2.5) using multi-leg Monte Carlo programs [24] so the strict EFT treatment is not necessary.

Also the non-resonant diagrams are in general well-defined only with kinematic cuts, as mentioned above. A study of the full non-resonant effects for all squark and gluino production processes would therefore require a dedicated study taking the realistic selection cuts used by the LHC experiments into account, which is beyond the scope of this work. We will therefore limit ourselves to an estimate of the unknown radiative corrections to the non-resonant contributions that cannot easily be computed in a Monte Carlo program. These are given by higher-order corrections to the diagrams shown in figure 4. The computation of these corrections is currently an ongoing effort for top-pair production at a linear collider [52, 53, 60, 61] and the computation for the case of squarks and gluinos is far beyond the scope of the present work. These corrections would also be included in a complete fixed-order NLO calculation of the process (2.5).

We consider again the two cases introduced in section 3.1:

a) Since in the calculation of the matching coefficients of the four-parton operator all the momenta are large compared to the scale δ, there is no enhancement of these corrections by resonant propagators and one expects them to be of the order [31]

$$\hat{\sigma}_{pp'}^{\text{non-res}} \sim \alpha_s^3 \sim \hat{\sigma}_{pp'}^{\text{res}} \times \frac{\alpha_s}{\beta}. \tag{3.10}$$

For the scaling (3.4) appropriate for $\Gamma/M \sim 10\%$, the leading non-resonant corrections are therefore of the order $\delta^{1/2} \sim \sqrt{\Gamma/M}$, as the first Coulomb correction. The unknown radiative corrections to the non-resonant contributions (3.10) therefore are of the order $\alpha_s\sqrt{\Gamma/M} \sim \alpha_s^{3/2}$ relative to the leading resonant cross section, and therefore beyond NLO accuracy.

b) For a small mass hierarchy leading to the scaling (3.6) the non-resonant contributions can be further expanded according to $\beta \ll \sqrt{\rho} \ll 1$, with $\rho = 1 - m/M$. For the case of top-quark production the leading non-resonant corrections were found to be of the order [53]

$$\hat{\sigma}_{pp'}^{\text{non-res}} \sim \hat{\sigma}_{pp'}^{\text{res}} \times \sqrt{\frac{\Gamma}{M\rho}}. \tag{3.11}$$

Using (3.5) we have

$$\frac{\Gamma}{M\rho} \sim \frac{\alpha_s(1-x^2)^\gamma}{(1-x)} \sim 2\alpha_s\kappa^{(\gamma-1)/\gamma}. \tag{3.12}$$

For squark and gluino decay $\gamma = 2$, so counting $\kappa \sim \alpha_s$ we find that the suppression of the non-resonant corrections is of the order of $(\frac{\Gamma}{M}\frac{1}{\alpha_s^{1/2}})^{1/2} \sim (\Gamma/M)^{3/8}$ compared to the leading resonant term. The unknown radiative non-resonant corrections are then of the order $(\frac{\Gamma}{M}\alpha_s^{3/2})^{1/2} \sim (\Gamma/M)^{7/8}$, i.e. of a similar magnitude as for the case $x \to 0$. These corrections are beyond NNLL accuracy.

To study the numerical impact of the non-resonant corrections, we consider the following approximations:

- $\hat{\sigma}_{\text{NWA}}^{(0)}$: The LO cross section calculated using the narrow-width approximation everywhere, i.e. the on-shell production cross section in the $\Gamma \to 0$ limit is multiplied by the decay branching ratios. This approximation is valid for $M \gg \Gamma$ and far above
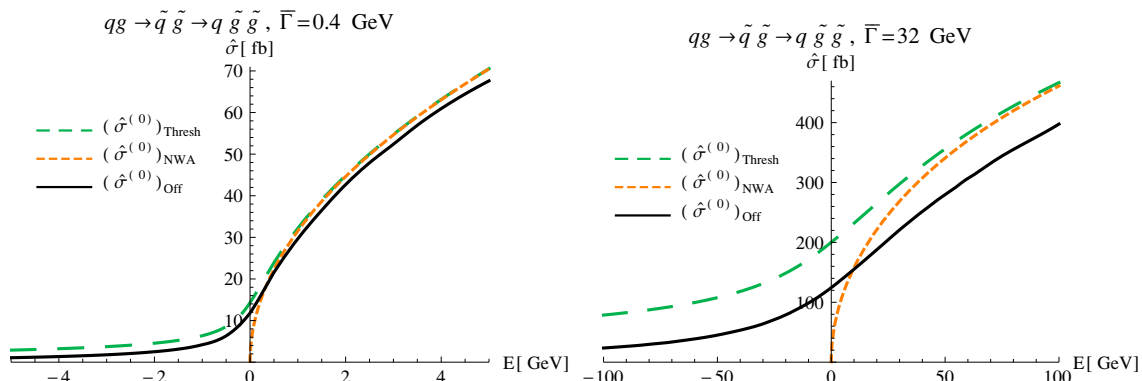
Figure 7. The partonic cross section for squark-gluino production and squark decay as a function of the energy $E = \bar{m}\beta^2$ at a fixed average mass $\bar{m} = \frac{1}{2}(m_{\tilde{q}} + m_{\tilde{g}}) = 1500\,\mathrm{GeV}$. Left: $r = \frac{m_{\tilde{g}}}{m_{\tilde{q}}} = 0.95, \bar{\Gamma} = 0.4\,\mathrm{GeV}$. Right: $r = 0.5, \bar{\Gamma} = 32\,\mathrm{GeV}$.

threshold [25]. In this work only the decay processes (2.3) are considered and thus $\hat{\sigma}_{\mathrm{NWA}}^{(0)} = \hat{\sigma}_{\mathrm{Tree}}^{(0)}(\Gamma = 0)$.

- $\hat{\sigma}_{\mathrm{Thresh}}^{(0)}$: The threshold approximated LO cross section in the EFT, using only the α_s^0 term of the potential function (2.17). The unstable-particle momentum in the centre of mass frame is in the potential region (slightly off-shell).

- $\hat{\sigma}_{\mathrm{Off}}^{(0)}$: The LO cross section obtained using the off-shell doubly-resonant diagrams and fixed-width Breit-Wigner propagators computed with WHIZARD [62] and validated with SHERPA [63] when possible. This implements tree-level off-shell effects and allows for unrestricted momenta of the unstable particles.[6]

In figure 7 the three different approximations of the partonic cross sections are shown for the example of squark-gluino production and subsequent squark decay as a function of the energy $E = \bar{m}\beta^2$ for two examples of the decay width. The plots for the other processes have the same behaviour as above and are not shown here. It can be seen that the EFT approximation $\hat{\sigma}_{\mathrm{Thresh}}^{(0)}$ agrees with the off-shell results for small widths, but is systematically shifted for larger decay width. This is the expected effect of the non-resonant contribution to the Born cross section, that is of the form $\hat{\sigma}_{pp'}^{\mathrm{non\text{-}res}} \sim \frac{\bar{m}^2}{\hat{s}} \mathrm{Im} C_{4p}$, and has also been observed in [31, 52, 60]. Note that while we do not include truly singly or non-resonant diagrams in the off-shell approximation, the off-shell momentum configurations of doubly-resonant diagrams contribute to the non-resonant part of the cross section and, in fact, provide the dominant numerical effect in the case of W or top production [31, 52, 53]. Therefore the shift observed in figure 7 provides an estimate of the non-resonant corrections. For $\bar{\Gamma}/\bar{m} = 32/1500 = 0.02$ the nonresonant correction is of the order of 40%, which is of the same order of magnitude, but somewhat larger, than the estimate $(\Gamma/M)^{1/2}$–$(\Gamma/M)^{3/8} = 14\%$–24%. We then estimate that the uncalculated corrections due to higher-order non-resonant effects are of the order of $\lesssim 5\%$.

---

[6]The selection of doubly-resonant diagrams violates gauge invariance. However, we have verified for a selection of different covariant and axial gauges that gauge violation is numerically below 1% for the processes of interest in this work.

4 Application to squark and gluino production at LHC

In this section we present results for finite-width effects on the soft and Coulomb NLL corrections to squark and gluino production at the LHC in the setup discussed in section 2. In section 4.1 we give results for the invariant-mass distributions, while in section 4.2 we discuss our implementation and present numerical results for the total cross sections.

4.1 Invariant-mass distributions

In order to discuss the finite-width effects on the production cross sections, we first consider the invariant-mass distribution. Similarly to the total cross section (2.12), it satisfies a factorization formula near the production threshold [11] (see also e.g. [21])

$$\frac{d\sigma_{NN'}^{\rm res}(\hat{s},\mu)}{dM_{\tilde{s}_1\tilde{s}_2}} = \sum_{R_\alpha} J_{R_\alpha}(M_{\tilde{s}_1\tilde{s}_2}-2\bar{m}+i\bar{\Gamma}) \sum_{p,p'=q,\bar{q},g} 2H_{pp'}^{R_\alpha}(\mu)\int_{\tau_0}^1 d\tau L_{pp'}(\tau,\mu)W^{R_\alpha}(2(\sqrt{\hat{s}}-M_{\tilde{s}_1\tilde{s}_2}),\mu),$$
(4.1)

where $\tau_0 = M_{\tilde{s}_1\tilde{s}_2}^2/s$. We have defined the parton luminosity in terms of the PDFs $f_{p/N}$ for a parton p in a nucleon N:

$$L_{pp'}(\tau,\mu) = \int_0^1 dx_1 dx_2\, \delta(x_1 x_2 - \tau)\, f_{p/N_1}(x_1,\mu) f_{p'/N_2}(x_2,\mu).$$
(4.2)

In our numerical results we use the NLL-resummed soft function that can be found in [12]. Since we are interested in the invariant-mass spectrum near threshold we deviate somewhat from the default treatment of the total cross section and always express the hard function in terms of the threshold-approximation of the Born cross section and use a constant Coulomb scale, defined as solution to the equation $\mu_C = 2\alpha_s(\mu_C)m_r|D_{R_\alpha}|$, and constant soft scales μ_s that are process-specific and determined in [12].

Consistent with the treatment of the total cross section discussed in section 2.3, as a default we use the expression (2.14) for the energy of the squark or gluino pair, i.e. we write the argument of the soft function W^{R_α} in (4.1) as

$$\sqrt{\hat{s}} - M_{\tilde{s}_1\tilde{s}_2} \to \bar{m}\left(1 - \frac{4\bar{m}^2}{\hat{s}}\right) + 2\bar{m} - M_{\tilde{s}_1\tilde{s}_2}.$$
(4.3)

As for the total cross section, this will be referred to as the 'β-implementation'. Note that the soft function vanishes for negative argument which implies that the lower boundary of the τ integral is given by

$$\tau_0 = \frac{4\bar{m}^2}{s}\frac{\bar{m}}{3\bar{m} - M_{\tilde{s}_1\tilde{s}_2}}.$$
(4.4)

In order to estimate ambiguities of our treatment, we also introduce an 'E-implementation' keeping the unexpanded expression $\sqrt{\hat{s}} - M_{\tilde{s}_1\tilde{s}_2}$ in the argument of the soft function. In order not to introduce artificial differences in the two implementations due to a different boundary of the τ integral, we perform the replacement $M_{\tilde{s}_1\tilde{s}_2} \to M'_{\tilde{s}_1\tilde{s}_2} \equiv \bar{m}(3 - 4\bar{m}^2/M_{\tilde{s}_1\tilde{s}_2}^2)$ in the E-implementation and consider the differential cross section with respect to $M'_{\tilde{s}_1\tilde{s}_2}$.

Based on experience with W-pair production [31] we do not expect the leading resonant approximation to be valid significantly below the nominal threshold, where higher-order
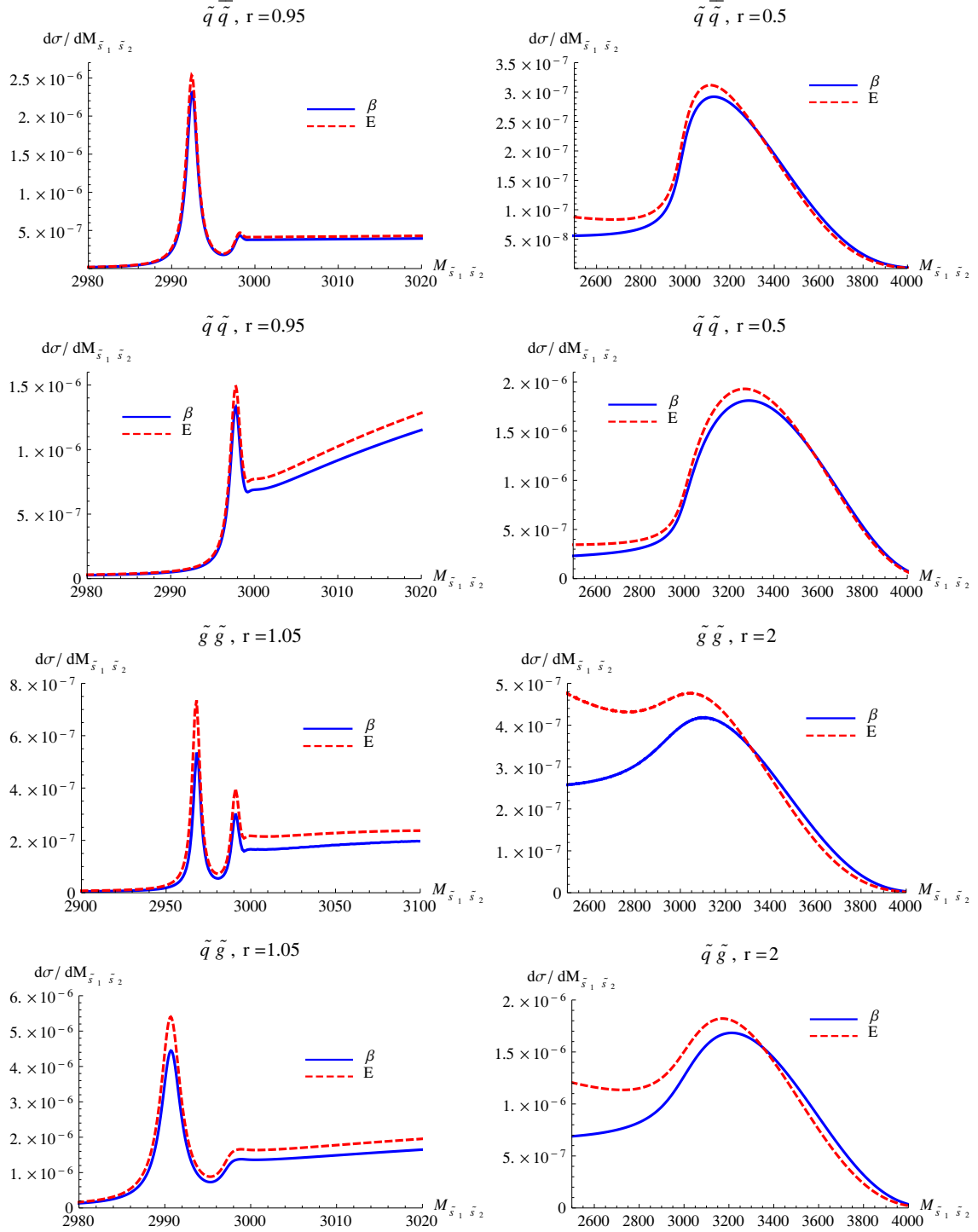
Figure 8. Invariant-mass distributions for an average mass $\bar{m} = 1500\,\text{GeV}$ of the produced sparticle pair and a centre-of-mass energy $\sqrt{s} = 8\,\text{TeV}$ for the β (blue, solid) and E (red, dashed) implementation as defined below (4.3). Left-hand plots are examples of case b) ($\bar{\Gamma}/\bar{m} \sim \alpha_s^2$), right-hand plots case a) ($\bar{\Gamma}/\bar{m} \sim \alpha_s$).

terms in the non-relativistic expansion and non-resonant contributions become important. The differences between the default β and the E approximation provide an estimate for the size of the higher-order relativistic effects. Note that because of soft radiation (as taken into account by the convolution of the soft function with the parton luminosity) also the invariant-mass distribution directly at threshold is sensitive to larger partonic centre-of-mass energies and the associated ambiguities in the threshold expansion.

In figure 8 the invariant-mass distributions for the four relevant squark and gluino production processes (2.6) are shown for $\bar{m} = 1500\,\text{GeV}$ at a centre-of-mass energy $\sqrt{s} = 8\,\text{TeV}$ for two different mass ratios corresponding to the cases a) and b) discussed in section 3.1 . For the case $m_{\tilde{g}} > m_{\tilde{q}}$ we consider $r = m_{\tilde{g}}/m_{\tilde{q}} = 2$ and $r = 1.05$, corresponding to $\Gamma_{\tilde{g}}/m_{\tilde{g}} = 12\%$ and $\Gamma_{\tilde{g}}/m_{\tilde{g}} = 0.2\%$, respectively. For the case $m_{\tilde{g}} < m_{\tilde{q}}$ we consider $r = 0.5$ and $r = 0.95$, corresponding to $\Gamma_{\tilde{q}}/m_{\tilde{q}} = 3\%$ and $\Gamma_{\tilde{q}}/m_{\tilde{q}} = 0.05\%$, respectively. As explained in section 3, we will perform treshold resummation also for the case of larger decay widths, although it might not be strictly necessary in this case.

In the small-width case, i.e. the left-hand plots in figure 8 where $r = 0.95$ or $r = 1.05$, the ambiguities in our prediction as estimated by the difference of the E- and β-implementations are moderate. Depending on the process, the different regimes mentioned in section 3.1 are observed: for the given choice of parameters, a single would-be bound-state peak appears for squark-squark production, where $\bar{\Gamma} = 0.9\,\text{GeV} \lesssim E_1 = 1.5\,\text{GeV}$, while two peaks are visible in gluino-pair production where $\bar{\Gamma} = 3\,\text{GeV} \ll E_1 = 30\,\text{GeV}$. In the remaining two processes the second bound-state peak is less pronounced, but still visible.

In the case of larger widths, i.e. the right-hand plots in figure 8 with $r = 0.5$ or $r = 2$, the decay widths are always much larger than the bound-state energy, so no peaks below threshold are observed. It can be seen that the invariant-mass distributions do not vanish for $M_{\tilde{s}_1 \tilde{s}_2}$ far below the nominal threshold, $M_{\tilde{s}_1 \tilde{s}_2} = 3000\,\text{GeV}$. This behaviour arises as a combination of the rise of the PDFs for small x and the behaviour of the potential function in 4.1, that scales as $J_{D_R} \propto \bar{\Gamma}/(2\bar{m} - M_{\tilde{s}_1 \tilde{s}_2})^{1/2} \rightarrow \bar{\Gamma}/(2\bar{m})^{1/2}$ for $M_{\tilde{s}_1 \tilde{s}_2} \rightarrow 0$, which follows from the LO (trivial) potential function (2.17). While for the default β-implementation the distributions approach a flat plateau far below threshold, in the E-implementation one observes a (clearly unphysical) rise for larger widths for processes involving gluinos.[7] In fact, as already pointed out, far below threshold the LO potential function is not expected to be a good approximation, and the inclusion of non-resonant contributions and relativistic corrections are needed for a realistic description of the invariant-mass distributions in this region, similar to what was seen for the partonic cross sections in figure 7.

The difference between the E- and β-implementations is amplified due to the soft function in (4.1), $W^{R_\alpha}(\omega) \sim \omega^{-1+2\eta}$ with $\eta < 0$. In the E-implementation the argument of the soft function (left-hand side of eq. (4.3)) approaches zero faster than the corresponding quantity in the β-implementation (right-hand side of eq. (4.3)) as the lower integration

---

[7]Note that this is not an artifact of our use of $M'_{\tilde{s}_1 \tilde{s}_2}$ for the E-implementation. In fact, for the original formula (4.1) an even stronger rise is observed, since smaller x values are probed in the parton luminosity due to smaller values of τ_0.

boundary τ_0 is approached, and the soft function W diverges faster.[8] If soft corrections are not taken into account, the soft function reduces to a delta function, $W^{R_\alpha}(\omega) \propto \delta(\omega)$. In this case we have observed a substantial reduction in the difference between the E- and β-implementation also for large widths.

From the results presented in this section we conclude that our approximation is reasonably accurate for processes with decay widths of the order of $\bar{\Gamma}/\bar{m} \lesssim 5\%$. As we will argue in section 4.2, this covers the phenomenologically-relevant MSSM parameter-space regions. Our effective-theory treatment becomes inadequate for larger decay widths, so our results in this regime should be considered as indicative only.

4.2 Total cross sections

In order to compute the total cross section for a finite decay width, in principle the ω-integral in (2.12) has to be performed up to the maximal energy $\omega = 2\sqrt{\hat{s}}$ since the potential function J_{R_α} is defined for arbitrary negative values of the partonic energy E. However, as mentioned above, far below threshold (i.e. $\omega \gg 2E$) the leading threshold approximation becomes insufficient and higher-order and non-resonant contributions become relevant. This was shown by the difference of the $\hat{\sigma}^{(0)}_{\text{thresh}}$ and $\hat{\sigma}^{(0)}_{\text{Off}}$ curves for large widths in figure 7 and by the large difference of the β- and E-implementations for the invariant-mass spectrum and the unphysical behaviour of the latter below threshold, as seen in figure 8. Since the non-resonant and higher-order non-relativistic corrections for squark and gluino production are not available beyond LO, we introduce a cut-off in the potential function:

$$J_R(E + i\bar{\Gamma}) = 2\text{Im}\left[G_R\left(E + i\bar{\Gamma}\right)\right]\theta\left(E + \Delta E\right), \quad \Delta E > 0, \tag{4.5}$$

with E equal to the expression (2.14) as our default implementation. The parameter ΔE cuts off the convolution of the soft and potential function at $\omega = 2(E + \Delta E)$. In order to capture the bound-state peaks, this cut-off is chosen as

$$\Delta E = 1.1|E_1| + \overline{\Delta E}, \tag{4.6}$$

where E_1 is the energy of the lowest-lying bound-state peak, see eq. (2.18). The prefactor 1.1 multiplying E_1 insures that the bound-state contribution is always fully included. As a default for $\overline{\Delta E}$ we take

$$\overline{\Delta E_0} := \text{Min}[10\,\bar{\Gamma}, 0.25\,\bar{m}]. \tag{4.7}$$

A related cutoff $\Delta E = |E_1| + 3\bar{\Gamma}$ was used for gluino-pair production in [21] where the focus was on narrow gluinos with decay widths at most of the order of $\Gamma_{\tilde{g}} \sim |E_1| \sim m_{\tilde{g}}\alpha_s^2$. In the case of larger decay widths, the value of $\Delta\overline{E} = 10\bar{\Gamma}$ becomes of the order of $m_{\tilde{g}}$, where we expect the threshold approximation to become invalid. Therefore we have chosen the cutoff $\overline{\Delta E} \sim 0.25\bar{m}$ in the case of larger decay widths. The uncertainty in choosing $\overline{\Delta E}$ is estimated by varying it around its default value:

$$\overline{\Delta E_0}/2 \leq \overline{\Delta E} \leq 2\overline{\Delta E_0}. \tag{4.8}$$

---

[8]This is further enhanced by the rise of the PDFs at the lower integration boundary.

The hadronic cross sections are obtained by convoluting the partonic cross sections with the parton luminosity (4.2)

$$\sigma_{N_1 N_2 \to \tilde{s}\tilde{s}'X}(s) = \int_{\tau_0}^1 d\tau \sum_{p,p'=q,\bar{q},g} L_{pp'}(\tau, \mu_f) \hat{\sigma}_{pp'}(\tau s, \mu_f), \qquad (4.9)$$

where the lower integration boundary depends on the cutoff,

$$\tau_0(\Delta E) = \frac{4\bar{m}^2}{s} \frac{1}{1 + \Delta E/\bar{m}}. \qquad (4.10)$$

In the E-implementation, the lower integration boundary is instead given by $\tau_0(\Delta E) = (2\bar{m} - \Delta E)^2/s$. In order not to introduce numerical differences due to different integration boundaries, in the E-implementation we use the same numerical value for τ_0 as for the β-implementation, and adjust the value of ΔE in the potential function accordingly.[9]

While the Born amplitudes for the production and decay processes of squarks and gluinos can be treated exactly with Monte Carlo programs [24], the NLO corrections for the production processes are known only in the narrow-width approximation, as implemented in Prospino [64]. In order to take these exactly-known contributions into account, we match our finite-width NLL results to the sum of the Born cross section including finite-width effects and the NLO corrections in the narrow-width approximation. In practice, we approximate the Born cross section by $\sigma_{\text{Off}}^{(0)}$ defined in section 3.4 and computed with Whizard. The total hadronic cross sections at NLO for finite widths are thus approximated as:

$$\sigma_{\text{NLO}}(\bar{\Gamma}) = \sigma_{\text{Off}}^{(0)}(\bar{\Gamma}) + (\sigma_{\text{NLO,NWA}} - \sigma_{\text{NWA}}^{(0)}). \qquad (4.11)$$

Here $\sigma_{\text{NLO,NWA}}$ is the NLO result obtained with Prospino and $\sigma_{\text{NWA}}^{(0)}$ is the leading-order production cross section for stable squarks or gluinos (see section 3.4). Analogously to the narrow-width case [12], the NLL resummed cross section is then matched to $\sigma_{\text{NLO}}(\bar{\Gamma})$:

$$\sigma_{\text{NLL}}^{\text{matched}}(\bar{\Gamma}) = \Delta\sigma_{\text{NLL}}(\bar{\Gamma}) + \sigma_{\text{NLO}}(\bar{\Gamma}),$$
$$\Delta\sigma_{\text{NLL}}(\bar{\Gamma}) = \sigma_{\text{NLL}}(\bar{\Gamma}) - \sigma_{\text{NLL, LO}}(\bar{\Gamma}) - \sigma_{\text{NLL, NLO}}(\bar{\Gamma} = 0). \qquad (4.12)$$

Here $\sigma_{\text{NLL, (N)LO}}$ is the expansion of the NLL resummed cross section to (N)LO accuracy. For comparison we will also consider results where the decay width is set to zero in the higher-order corrections, i.e.

$$\sigma_{\text{NLL}}^{\text{matched}}(0) = \Delta\sigma_{\text{NLL}}(0) + \sigma_{\text{NLO}}(\bar{\Gamma}). \qquad (4.13)$$

The result (4.12) is our best current prediction. It could be made more realistic by replacing the off-shell approximation for the tree cross section by a full LO simulation including acceptance cuts, which we leave for further investigation. Contrary to the NLO cross section $\sigma_{\text{NLO}}(\bar{\Gamma})$, the matched NLL cross section $\sigma_{\text{NLL}}(\bar{\Gamma})$ does contain finite-width effects at NLO from the resummed Coulomb and soft corrections. It is also interesting to consider

---

[9]This is related to the replacement of the invariant mass $M_{\tilde{s}_1\tilde{s}_2} \to M'_{\tilde{s}_1\tilde{s}_2}$ for the E-implementation in section 4.1.
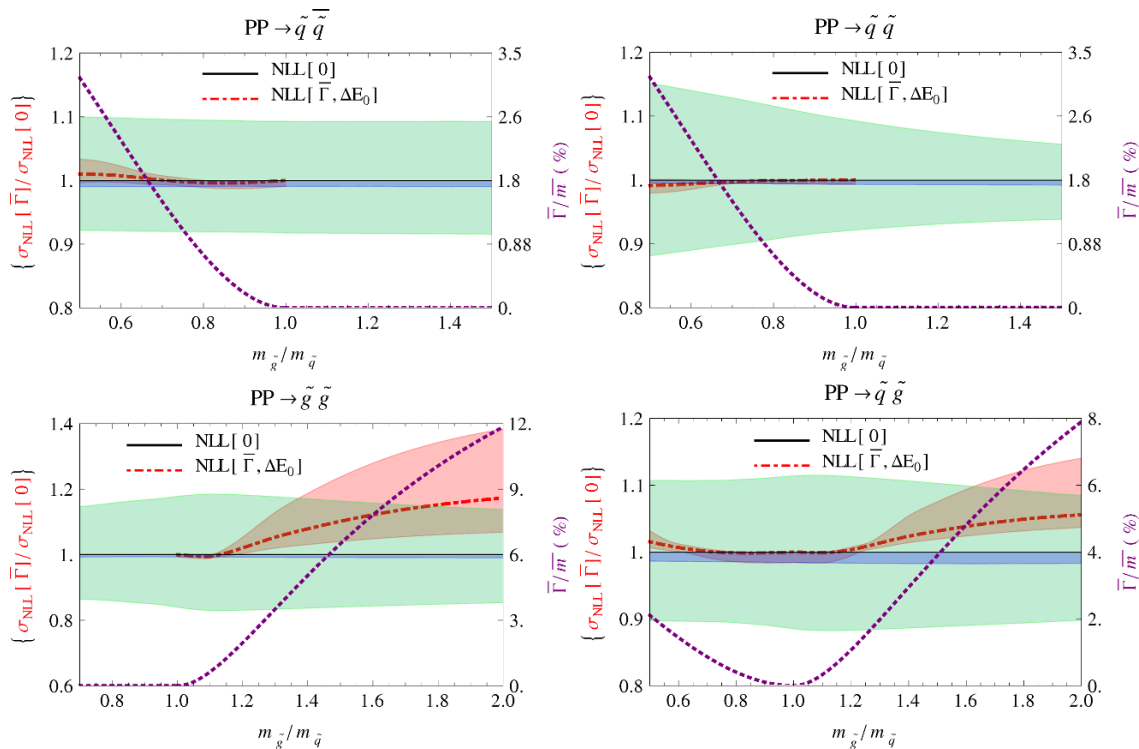
Figure 9. The plots show the ratio $\sigma_{\mathrm{NLL}}^{\mathrm{matched}}(\bar{\Gamma})/\sigma_{\mathrm{NLL}}^{\mathrm{matched}}(0)$ of the matched finite-width NLL cross section (4.12) to the zero-width approximation (4.13) (red dot-dashed, left-hand vertical axis) for $\bar{m} = 1500\,\mathrm{GeV}$ and $\sqrt{s} = 8\,\mathrm{TeV}$ and the ratio $\bar{\Gamma}/\bar{m}$ in per-cent (purple dotted, right-hand vertical axis). Both quantities are plotted as a function of the gluino-to-squark mass ratio. The NLL result is for default $\Delta E = \Delta E_0$. The red band represents the error from $\overline{\Delta E}$ variation and E vs β uncertainty added in quadrature, the green band the total error for zero width, the blue band the E vs β uncertainty for the zero-width case.

only the finite-width corrections beyond NLO. This shows the size of the effects that are beyond a possible future exact NLO calculation of the processes (2.6). For this purpose we consider the alternative matching

$$
\begin{aligned}
\sigma_{\mathrm{NLL}}^{\mathrm{matched},(2)}(\bar{\Gamma}) &= \Delta\sigma_{\mathrm{NLL}}^{(2)}(\bar{\Gamma}) + \sigma_{\mathrm{NLO}}(\bar{\Gamma}), \\
\Delta\sigma_{\mathrm{NLL}}^{(2)}(\bar{\Gamma}) &= \sigma_{\mathrm{NLL}}(\bar{\Gamma}) - \sigma_{\mathrm{NLL,\,LO}}(\bar{\Gamma}) - \sigma_{\mathrm{NLL,\,NLO}}(\bar{\Gamma}).
\end{aligned} \tag{4.14}
$$

For the results shown in this section we take as a representative average mass $\bar{m} = 1500\,\mathrm{GeV}$ and the setting is the LHC at a centre-of-mass energy of $\sqrt{s} = 8\,\mathrm{TeV}$. We use the β-implementation as default and the scales are taken to be the same as in the zero-width case [12]: $\mu_f = \bar{m} = 1500\,\mathrm{GeV}$, $\mu_h = 2\bar{m} = 3000\,\mathrm{GeV}$ and a running soft and Coulomb scale. We note that the soft and Coulomb scales are always fixed below threshold. The LO widths in eq. (2.4) for the squarks and gluinos are used.

Figure 9 shows the ratio of the matched NLL cross section for finite widths (4.12) to that for the zero-width case (4.13) (red, dot-dashed) as a function of the gluino-to-squark mass ratio. The green band gives the total uncertainty for the zero-width NLL
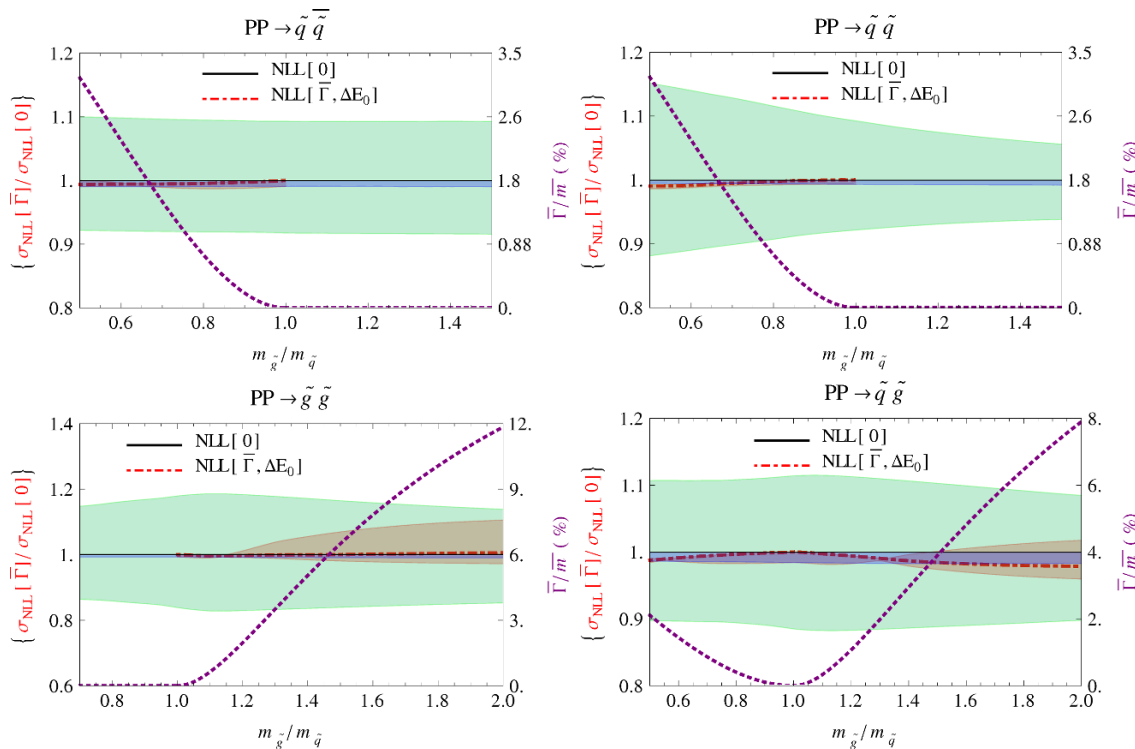
Figure 10. Same as in figure 9, but for the ratio $\sigma_{\mathrm{NLL}}^{\mathrm{matched},(2)}(\bar{\Gamma})/\sigma_{\mathrm{NLL}}^{\mathrm{matched}}(0)$ of the matched cross section (4.14) including only finite-width effects beyond NLO to the zero-width approximation (4.13). See figure 9 and the text for explanation.

result, including ambiguities in soft, hard, factorization and Coulomb-scale choices and the difference of the E- and β-implementation, added up in quadrature as discussed in detail in [12]. The difference of the E- and β-implementation alone is given by the blue band. The red band indicates the ambiguities related to our implementation of the finite-width effects, as estimated by the $\overline{\Delta E}$ variation as described in eq. (4.8) and the difference of the E- and β-implementations, summed in quadrature. The plots also show the ratio of the average decay width to the average mass of the produced particles.

It can be seen that for all processes the finite-width result including uncertainties lies within the uncertainty estimate of the NLL calculation for stable squarks and gluinos if $\bar{\Gamma}/\bar{m} \lesssim 5\%$. For larger widths, large corrections are observed for the gluino-gluino and squark-gluino processes, where the ratio $\bar{\Gamma}/\bar{m}$ grows up to 12%, and the finite-width corrections become of the order of 20%. In this case the uncertainties due to the treatment of finite-width effects are of a similar magnitude as those due to scale and resummation ambiguities. This indicates that corrections beyond the leading $E \to E + i\bar{\Gamma}$ replacement, such as higher-order non-relativistic corrections and non-resonant corrections become relevant. A more accurate treatment would require the matching of the NLL results to the exact NLO QCD cross sections for the full $\tilde{q}\tilde{q}q$ or $\tilde{q}\tilde{q}qq$-processes and the inclusion of the $\mathrm{N}^{3/2}\mathrm{LO}$ corrections in the counting (3.9) that are expected to be of the order $\delta^{3/2} \sim (\bar{\Gamma}/\bar{m})^{3/2} \sim 5\%$, both of which are not available at the moment. Nevertheless it is interesting to anticipate such a future matching to a full NLO calculation by using the matching prescription (4.14)
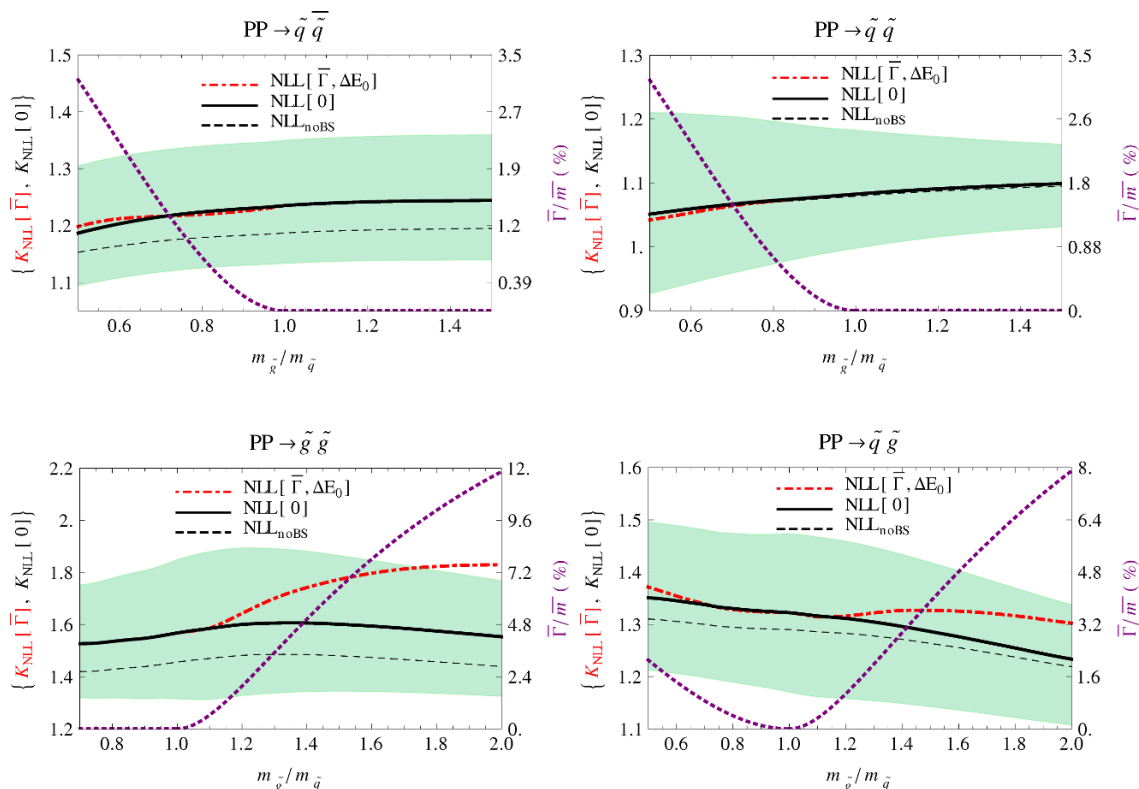
– 22 –

Figure 11. The K-factors of the NLL cross sections including (red dot-dashed) and excluding (black) the widths for default $\Delta E = \Delta E_0$ and $\bar{m} = 1500\,\text{GeV}$ at centre of mass energy $\sqrt{s} = 8\,\text{TeV}$. Dashed black: NLL resummed cross sections excluding bound-state contributions. Green band: Total error for zero width.

where the finite-width effects are included purely beyond NLO. The results are shown in figure 10, where the colour coding used for the lines is the same as in figure 9. It is seen that the finite-width effects on the central values, as well as ambiguities due to the ΔE variation and the E- and β-implementation difference, are much smaller than for the matching (4.12). In particular, the total uncertainty bands related to the finite-width implementation (red) lie now fully within the total zero-width NLL error bands (green). The difference of the plots in figure 9 and figure 10 indicates the potential impact of a full NLO SQCD calculation for the processes (2.6) and shows that the finite-width effects beyond NLO are expected to be small.

To assess the size of the finite width corrections relative to the NLL soft and Coulomb corrections, in figure 11 we compare the K-factors for our NLL result including finite decay widths to the result for stable squarks and gluinos (4.13). The K-factors relative to the NLO prediction are defined as $K_{\text{NLL}} = \sigma_{\text{NLL}}/\sigma_{\text{NLO}}$, where the finite-width approximation (4.11) is always used for the denominator. We also show the result NLL_{noBS} defined as the cross section in the stable case, excluding the bound-state contribution below threshold. In general, for relatively narrow particles with $\bar{\Gamma}/\bar{m} \lesssim 5\%$ the K-factors including finite-width effects are well approximated by those for the zero-width case including the bound-state
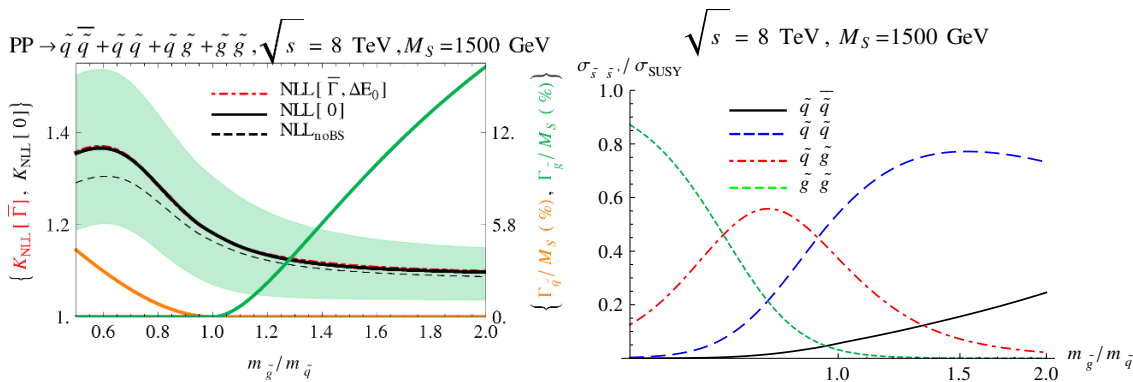
Figure 12. Left plot: The NLL K-factor including (dot-dashed red) and excluding (black) the widths for default $\Delta E = \Delta E_0$ and $M_S = (m_{\tilde{q}} + m_{\tilde{g}})/2 = 1500$ GeV at centre of mass energy $\sqrt{s} = 8$ TeV. Dashed black: NLL K-factor excluding bound-state contributions. Green band: Total error for zero width. The plot also shows the squark (thick orange) and gluino (thick green) widths (right vertical axis). Right plot: The ratio of the four relevant NLL cross sections to the total SUSY cross section.
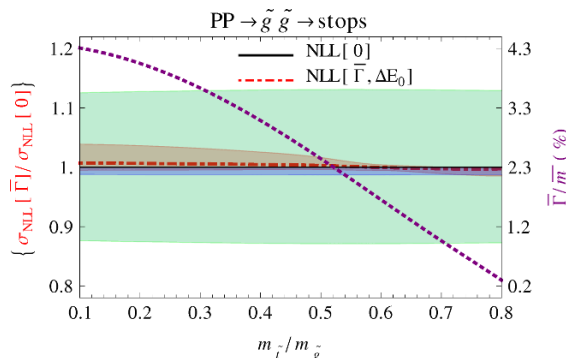

Figure 13. Ratio of the matched finite-width NLL cross section (4.12) to the zero-width approximation (4.13) for gluino-pair production and subsequent decay to stops, as a function of $m_{\tilde{t}}/m_{\tilde{g}}$ for a fixed gluino mass $m_{\tilde{g}} = 1000$ GeV, a common light-flavour squark mass of $m_{\tilde{q}} = 2000$ GeV. The error bands for finite- and zero-width curves are defined as in figures 9 and 10.

contribution, with the exception of squark-gluino production and gluino-gluino production for the case $m_{\tilde{g}} > m_{\tilde{q}}$, where larger finite-width effects are observed.

The relatively large finite-width corrections for gluino-production processes for $m_{\tilde{g}} > m_{\tilde{q}}$ have to be compared to the contributions of these processes to the total SUSY production rate. This can be seen in figure 12, where in the left plot the K_{NLL}-factor is shown for the finite-width and zero-width case. The effect of the QCD widths is seen to be negligible and the finite width can be safely set to zero when it comes to the total SUSY cross section. This is also expected since the numerically dominant processes are almost always those whose final-state particles are stable against SQCD decay, as can be seen from the right plot of figure 12. The inclusion of electroweak widths is not expected to change our qualitative results. These can be dominating when $r \simeq 1$, but are only about the order of $\bar{\Gamma}/\bar{m} \sim 1\%$ and thus the effects are expected to be negligible.

As mentioned in section 2, in the study of finite-width effects considered in this work we have neglected the decay of gluinos to stops. We do not expect the inclusion of this

additional decay channel to significantly change the results presented in this section, except in the case in which gluino production is the dominant SUSY production channel and the gluinos only decay to stops. This is for example the case of scenarios with the mass hierarchy $m_{\tilde{t}} < m_{\tilde{g}} \ll m_{\tilde{q}}$, with all squarks heavy except for stops. To have an estimate of the effects of a finite gluino width in this particular situation in figure 13 we show the NLL cross section for gluino-gluino production as a function of the ratio $m_{\tilde{t}}/m_{\tilde{g}}$ for a fixed gluino mass $m_{\tilde{g}} = 1000\,\mathrm{GeV}$, a common light-flavour squark mass of $m_{\tilde{q}} = 2000\,\mathrm{GeV}$ and top mass $m_t = 174\,\mathrm{GeV}$. As in figure 9 the cross section is normalized to the gluino-pair production cross section at zero width, and the green band represents the total uncertainty of the zero-width result, while the purple dashed curve gives the gluino width as a function of $m_{\tilde{t}}/m_{\tilde{g}}$. As can be seen from the plot the finite-width effects amount to a maximum of $\sim 1 - 2\%$ for small stop masses and the uncertainty associated with the finite-width result is contained in the zero-width case error band. We thus expect corrections to the plots in figures 11, 12 to amount to at most few percents.

5 Conclusions

In this work we have considered corrections related to finite widths of squarks and gluinos on the NLL resummed results presented in [12]. As anticipated, a finite decay width leads to a screening of higher-order soft and Coulomb corrections. However we have found that for decay widths of the order of $\bar{\Gamma}/\bar{m} \lesssim 5\%$, corresponding to gluino to squark mass ratios of $0.5 \lesssim m_{\tilde{g}}/m_{\tilde{q}} \lesssim 1.4$, finite-width effects on the NLL corrections are small and within the uncertainty of the soft and Coulomb resummation including bound-state effects performed in [12].

For larger decay widths of the order of $\bar{\Gamma}/\bar{m} \sim \alpha_s$ non-resonant contributions and higher order non-relativistic corrections become important. In this case it becomes necessary to perform a calculation of order $\delta^{3/2} \sim \alpha_s\sqrt{\bar{\Gamma}/\bar{m}}$ in unstable particle-effective theory matched to an exact NLO calculation for three- or four-particle final states including finite-width effects, which should be feasible but challenging with current NLO technology. The accuracy of such a calculation is expected to be better than 5%. For the doubly-resonant contributions to the cross section, we have observed that finite-width corrections beyond NLO are small.

Because the pair production processes of the lighter coloured sparticles, which are stable with respect to SQCD, dominate the total SUSY cross section, finite-width effects on the total SUSY production rate are negligible on the whole range of squark and gluino widths considered.

References

[1] A. Kulesza and L. Motyka, *Threshold resummation for squark-antisquark and gluino-pair production at the LHC*, *Phys. Rev. Lett.* **102** (2009) 111802 [arXiv:0807.2405] [INSPIRE].

[2] A. Kulesza and L. Motyka, *Soft gluon resummation for the production of gluino-gluino and squark-antisquark pairs at the LHC*, *Phys. Rev.* **D 80** (2009) 095004 [arXiv:0905.4749] [INSPIRE].

[3] W. Beenakker, S. Brensing, M. Krämer, A. Kulesza, E. Laenen, et al., *Soft-gluon resummation for squark and gluino hadroproduction*, *JHEP* **12** (2009) 041 [arXiv:0909.4418] [INSPIRE].

[4] W. Beenakker, S. Brensing, M. Krämer, A. Kulesza, E. Laenen, et al., *Supersymmetric top and bottom squark production at hadron colliders*, *JHEP* **08** (2010) 098 [arXiv:1006.4771] [INSPIRE].

[5] W. Beenakker, S. Brensing, M. Krämer, A. Kulesza, E. Laenen, et al., *NNLL resummation for squark-antisquark pair production at the LHC*, *JHEP* **01** (2012) 076 [arXiv:1110.2446] [INSPIRE].

[6] U. Langenfeld and S.-O. Moch, *Higher-order soft corrections to squark hadro-production*, *Phys. Lett.* **B 675** (2009) 210 [arXiv:0901.0802] [INSPIRE].

[7] U. Langenfeld, *Threshold improved QCD corrections for stop-antistop production at hadron colliders*, *JHEP* **07** (2011) 052 [arXiv:1011.3341] [INSPIRE].

[8] U. Langenfeld, S.-O. Moch and T. Pfoh, *QCD threshold corrections for gluino pair production at hadron colliders*, *JHEP* **11** (2012) 070 [arXiv:1208.4281] [INSPIRE].

[9] M. Beneke, P. Falgari and C. Schwinn, *Soft radiation in heavy-particle pair production: all-order colour structure and two-loop anomalous dimension*, *Nucl. Phys.* **B 828** (2010) 69 [arXiv:0907.1443] [INSPIRE].

[10] M. Beneke, P. Falgari and C. Schwinn, *Colour structure in threshold resummation and squark-antisquark production at NLL*, *PoS* **EPS-HEP2009** (2009) 319 [arXiv:0909.3488] [INSPIRE].

[11] M. Beneke, P. Falgari and C. Schwinn, *Threshold resummation for pair production of coloured heavy (s)particles at hadron colliders*, *Nucl. Phys.* **B 842** (2011) 414 [arXiv:1007.5414] [INSPIRE].

[12] P. Falgari, C. Schwinn and C. Wever, *NLL soft and Coulomb resummation for squark and gluino production at the LHC*, *JHEP* **06** (2012) 052 [arXiv:1202.2260] [INSPIRE].

[13] G.F. Sterman, *Summation of large corrections to short distance hadronic cross-sections*, *Nucl. Phys.* **B 281** (1987) 310 [INSPIRE].

[14] S. Catani and L. Trentadue, *Resummation of the QCD perturbative series for hard processes*, *Nucl. Phys.* **B 327** (1989) 323 [INSPIRE].

[15] N. Kidonakis and G.F. Sterman, *Resummation for QCD hard scattering*, *Nucl. Phys.* **B 505** (1997) 321 [hep-ph/9705234] [INSPIRE].

[16] R. Bonciani, S. Catani, M.L. Mangano and P. Nason, *NLL resummation of the heavy quark hadroproduction cross-section*, *Nucl. Phys.* **B 529** (1998) 424 [*Erratum ibid.* **B 803** (2008) 234] [hep-ph/9801375] [INSPIRE].

[17] V.S. Fadin and V.A. Khoze, *Threshold behavior of heavy top production in e^+e^- collisions*, *JETP Lett.* **46** (1987) 525 [ɪɴSPIRE].

[18] M.R. Kauth, J.H. Kuhn, P. Marquard and M. Steinhauser, *Gluinonia: energy levels, production and decay*, *Nucl. Phys.* **B 831** (2010) 285 [arXiv:0910.2612] [ɪɴSPIRE].

[19] J.E. Younkin and S.P. Martin, *QCD corrections to stoponium production at hadron colliders*, *Phys. Rev.* **D 81** (2010) 055006 [arXiv:0912.4813] [ɪɴSPIRE].

[20] I.I. Bigi, V.S. Fadin and V.A. Khoze, *Stop near threshold*, *Nucl. Phys.* **B 377** (1992) 461 [ɪɴSPIRE].

[21] K. Hagiwara and H. Yokoya, *Bound-state effects on gluino-pair production at hadron colliders*, *JHEP* **10** (2009) 049 [arXiv:0909.3204] [ɪɴSPIRE].

[22] M.R. Kauth, J.H. Kuhn, P. Marquard and M. Steinhauser, *Gluino pair production at the LHC: the threshold*, *Nucl. Phys.* **B 857** (2012) 28 [arXiv:1108.0361] [ɪɴSPIRE].

[23] M.R. Kauth, A. Kress and J.H. Kuhn, *Gluino-squark production at the LHC: the threshold*, *JHEP* **12** (2011) 104 [arXiv:1108.0542] [ɪɴSPIRE].

[24] K. Hagiwara, W. Kilian, F. Krauss, T. Ohl, T. Plehn, et al., *Supersymmetry simulations with off-shell effects for CERN LHC and ILC*, *Phys. Rev.* **D 73** (2006) 055005 [hep-ph/0512260] [ɪɴSPIRE].

[25] D. Berdine, N. Kauer and D. Rainwater, *Breakdown of the narrow width approximation for new physics*, *Phys. Rev. Lett.* **99** (2007) 111601 [hep-ph/0703058] [ɪɴSPIRE].

[26] C. Uhlemann and N. Kauer, *Narrow-width approximation accuracy*, *Nucl. Phys.* **B 814** (2009) 195 [arXiv:0807.4112] [ɪɴSPIRE].

[27] M. Gigg and P. Richardson, *Simulation of finite width effects in physics beyond the standard model*, arXiv:0805.3037 [ɪɴSPIRE].

[28] W. Hollik, J.M. Lindert and D. Pagani, *NLO corrections to squark-squark production and decay at the LHC*, arXiv:1207.1071 [ɪɴSPIRE].

[29] M. Beneke, A. Chapovsky, A. Signer and G. Zanderighi, *Effective theory approach to unstable particle production*, *Phys. Rev. Lett.* **93** (2004) 011602 [hep-ph/0312331] [ɪɴSPIRE].

[30] M. Beneke, A. Chapovsky, A. Signer and G. Zanderighi, *Effective theory calculation of resonant high-energy scattering*, *Nucl. Phys.* **B 686** (2004) 205 [hep-ph/0401002] [ɪɴSPIRE].

[31] M. Beneke, P. Falgari, C. Schwinn, A. Signer and G. Zanderighi, *Four-fermion production near the W pair production threshold*, *Nucl. Phys.* **B 792** (2008) 89 [arXiv:0707.0773] [ɪɴSPIRE].

[32] S. Actis, M. Beneke, P. Falgari and C. Schwinn, *Dominant NNLO corrections to four-fermion production near the W-pair production threshold*, *Nucl. Phys.* **B 807** (2009) 1 [arXiv:0807.0102] [ɪɴSPIRE].

[33] W. Beenakker, R. Hopker and P. Zerwas, *SUSY QCD decays of squarks and gluinos*, *Phys. Lett.* **B 378** (1996) 159 [hep-ph/9602378] [ɪɴSPIRE].

[34] H. Baer, V.D. Barger, D. Karatas and X. Tata, *Detecting gluinos at hadron supercolliders*, *Phys. Rev.* **D 36** (1987) 96 [ɪɴSPIRE].

[35] H. Baer, X. Tata and J. Woodside, *Phenomenology of gluino decays via loops and top quark Yukawa coupling*, *Phys. Rev.* **D 42** (1990) 1568 [ɪɴSPIRE].

[36] W. Porod, *SPheno, a program for calculating supersymmetric spectra, SUSY particle decays and SUSY particle production at e^+e^- colliders*, *Comput. Phys. Commun.* **153** (2003) 275 [hep-ph/0301101] [INSPIRE].

[37] W. Porod and F. Staub, *SPheno 3.1: extensions including flavour, CP-phases and models beyond the MSSM*, *Comput. Phys. Commun.* **183** (2012) 2458 [arXiv:1104.1573] [INSPIRE].

[38] M. Muhlleitner, A. Djouadi and Y. Mambrini, *SDECAY: a Fortran code for the decays of the supersymmetric particles in the MSSM*, *Comput. Phys. Commun.* **168** (2005) 46 [hep-ph/0311167] [INSPIRE].

[39] A. Djouadi, M. Muhlleitner and M. Spira, *Decays of supersymmetric particles: the program SUSY-HIT (SUspect-SdecaY-HDECAY-InTerface)*, *Acta Phys. Polon.* **B 38** (2007) 635 [hep-ph/0609292] [INSPIRE].

[40] A. Denner, S. Dittmaier, S. Kallweit and S. Pozzorini, *NLO QCD corrections to WWbb production at hadron colliders*, *Phys. Rev. Lett.* **106** (2011) 052001 [arXiv:1012.3975] [INSPIRE].

[41] G. Bevilacqua, M. Czakon, A. van Hameren, C.G. Papadopoulos and M. Worek, *Complete off-shell effects in top quark pair hadroproduction with leptonic decay at next-to-leading order*, *JHEP* **02** (2011) 083 [arXiv:1012.4230] [INSPIRE].

[42] D. Goncalves-Netto, D. Lopez-Val, K. Mawatari, T. Plehn and I. Wigmore, *Automated squark and gluino production to next-to-leading order*, arXiv:1211.0286 [INSPIRE].

[43] R.G. Stuart, *Gauge invariance, analyticity and physical observables at the Z^0 resonance*, *Phys. Lett.* **B 262** (1991) 113 [INSPIRE].

[44] A. Aeppli, G.J. van Oldenborgh and D. Wyler, *Unstable particles in one loop calculations*, *Nucl. Phys.* **B 428** (1994) 126 [hep-ph/9312212] [INSPIRE].

[45] V.S. Fadin, V.A. Khoze and A.D. Martin, *Interference radiative phenomena in the production of heavy unstable particles*, *Phys. Rev.* **D 49** (1994) 2247 [INSPIRE].

[46] K. Melnikov and O.I. Yakovlev, *Top near threshold: all α_s corrections are trivial*, *Phys. Lett.* **B 324** (1994) 217 [hep-ph/9302311] [INSPIRE].

[47] W. Beenakker, R. Hopker, M. Spira and P. Zerwas, *Squark and gluino production at hadron colliders*, *Nucl. Phys.* **B 492** (1997) 51 [hep-ph/9610490] [INSPIRE].

[48] C.W. Bauer, S. Fleming, D. Pirjol and I.W. Stewart, *An effective field theory for collinear and soft gluons: heavy to light decays*, *Phys. Rev.* **D 63** (2001) 114020 [hep-ph/0011336] [INSPIRE].

[49] C.W. Bauer, D. Pirjol and I.W. Stewart, *Soft collinear factorization in effective field theory*, *Phys. Rev.* **D 65** (2002) 054022 [hep-ph/0109045] [INSPIRE].

[50] M. Beneke, A. Chapovsky, M. Diehl and T. Feldmann, *Soft collinear effective theory and heavy to light currents beyond leading power*, *Nucl. Phys.* **B 643** (2002) 431 [hep-ph/0206152] [INSPIRE].

[51] N. Brambilla, A. Pineda, J. Soto and A. Vairo, *Potential NRQCD: an effective theory for heavy quarkonium*, *Nucl. Phys.* **B 566** (2000) 275 [hep-ph/9907240] [INSPIRE].

[52] M. Beneke, B. Jantzen and P. Ruiz-Femenia, *Electroweak non-resonant NLO corrections to $e^+e^- \to W^+W^-B\bar{b}$ in the $t\bar{t}$ resonance region*, *Nucl. Phys.* **B 840** (2010) 186 [arXiv:1004.2188] [INSPIRE].

[53] A.A. Penin and J.H. Piclum, *Threshold production of unstable top*, *JHEP* **01** (2012) 034 [arXiv:1110.1970] [INSPIRE].

[54] T. Becher and M. Neubert, *Infrared singularities of QCD amplitudes with massive partons*, *Phys. Rev.* **D 79** (2009) 125004 [*Erratum ibid.* **D 80** (2009) 109901] [arXiv:0904.1021] [INSPIRE].

[55] M. Czakon, A. Mitov and G.F. Sterman, *Threshold resummation for top-pair hadroproduction to next-to-next-to-leading log*, *Phys. Rev.* **D 80** (2009) 074017 [arXiv:0907.1790] [INSPIRE].

[56] T. Becher and M. Neubert, *Threshold resummation in momentum space from effective field theory*, *Phys. Rev. Lett.* **97** (2006) 082001 [hep-ph/0605050] [INSPIRE].

[57] E.H. Wichmann and C.-H. Woo, *Integral representation for the nonrelativistic Coulomb Green's function*, *J. Math. Phys.* **2** (1961) 178.

[58] M. Beneke, *Perturbative heavy quark-anti-quark systems*, hep-ph/9911490 [INSPIRE].

[59] Y. Kats and M.D. Schwartz, *Annihilation decays of bound states at the LHC*, *JHEP* **04** (2010) 016 [arXiv:0912.0526] [INSPIRE].

[60] A.H. Hoang, C.J. Reisser and P. Ruiz-Femenia, *Phase space matching and finite lifetime effects for top-pair production close to threshold*, *Phys. Rev.* **D 82** (2010) 014005 [arXiv:1002.3223] [INSPIRE].

[61] P. Ruiz-Femenia, *Non-resonant effects in the top-antitop resonance region*, arXiv:1203.0934 [INSPIRE].

[62] W. Kilian, T. Ohl and J. Reuter, *WHIZARD: simulating multi-particle processes at LHC and ILC*, *Eur. Phys. J.* **C 71** (2011) 1742 [arXiv:0708.4233] [INSPIRE].

[63] T. Gleisberg, S. Hoeche, F. Krauss, M. Schonherr, S. Schumann, et al., *Event generation with SHERPA 1.1*, *JHEP* **02** (2009) 007 [arXiv:0811.4622] [INSPIRE].

[64] W. Beenakker, R. Hopker and M. Spira, *PROSPINO: a program for the production of supersymmetric particles in next-to-leading order QCD*, hep-ph/9611232 [INSPIRE].